การประยุกต์ทฤษฎีฟังก์ชันนัลความหนาแน่นสำหรับควอนตัมดอทแบบวงกลม

นางสาว ขัตติยา ชลาพัฒน์

วิทยานิพนธ์นี้เป็นส่วนหนึ่งของการศึกษาตามหลักสูตรปริญญาวิทยาศาสตรมหาบัณฑิต
สาขาวิชาฟิสิกส์ ภาควิชาฟิสิกส์
คณะวิทยาศาสตร์ จุฬาลงกรณ์มหาวิทยาลัย
ปีการศึกษา 2545

ISBN 974-17-2892-1

APPLICATION OF DENSITY FUNCTIONAL THEORY FOR A CIRCULAR QUANTUM DOT

Miss Khattiya Chalapat

A Thesis Submitted in Partial Fulfillment of the Requirements
for the Degree of Master of Science in Physics

Department of Physics
Faculty of Science
Chulalongkorn University

Academic Year 2002
ISBN 974-17-2892-1

Thesis Title	Application of Density Functional Theory for a Circular Quantum Dot
By	Khattiya Chalapat
Field of Study	Physics
Thesis Advisor	Assoc. Prof. Wichit Sritrakool, Ph.D.

Accepted by the Faculty of Science, Chulalongkorn University in Partial Fulfillment of the Requirements for the Master 's Degree

…….. Dean of Faculty of Science
(Associate Professor Wanchai Phothiphichitr, Ph.D.)

THESIS COMMITTEE

…….. Chairman
(Assistant Professor Pisistha Ratanavararak, Ph. D.)

…….. Thesis Advisor
(Associate Professor Wichit Sritrakool, Ph.D.)

…….. Member
(Associate Professor Mayuree Natenapit, Ph.D.)

…….. Member
(Associate Professor Vudhichai Parasuk, Ph.D.)

ขัตติยา ชลาพัฒน์ : การประยุกต์ทฤษฎีฟังก์ชันนัลความหนาแน่นกับควอมตัมดอทแบบวงกลม (Application of Density Functional Theory for a Circular Quantum Dot) อ. ที่ปรึกษา : รศ. ดร. วิชิต ศรีตระกูล, จำนวนหน้า 90 หน้า. ISBN 974-17-2892-1.

วัตถุประสงค์ของวิทยานิพนธ์ คือ การศึกษาโครงสร้างสถานะของควอนตัมดอทโดยใช้ทฤษฎีฟังก์ชันนัลความหนาแน่นภายใต้การประมาณแบบความหนาแน่นอิเล็กตรอนเฉพาะที่ ในที่นี้เราใช้สูตรเชิงวิเคราะห์ของฟังก์ชันนัลพลังงานการแลกเปลี่ยนและสหสัมพันธ์ใหม่ของแอกคาตาไลท์และผู้ร่วมวิจัยแทนฟังก์ชันนัลเดิมของทานาตะและเซเพอร์ลี นอกจากนี้ยังได้ทำการวิเคราะห์ผลกระทบของศักย์ภายนอกและปฏิกิริยาระหว่างอิเล็กตรอนภายในควอนตัมดอทด้วย จากผลการคำนวณสำหรับศักย์แบบฮาร์โมนิก พบว่าพลังงานการเพิ่มอิเล็กตรอนจะมีค่าสูงมากเมื่ออิเล็กตรอนมีจำนวนเท่ากับ 2, 6 และ 12 ตัว และจะมีค่าค่อนข้างมากเมื่ออิเล็กตรอนมีจำนวนเท่ากับ 4 และ 9 ตัว และเพื่อศึกษาความสัมพันธ์ระหว่างสมมาตรของควอนตัมดอทกับโครงสร้างสถานะ เราได้ทำการคำนวณโดยใช้ศักย์ภายนอกแบบพาราโบลิก จากผลการคำนวณพบว่า ค่าพลังงานการเพิ่มอิเล็กตรอนมีค่าต่อเนื่องมากขึ้นเมื่อศักย์ภายนอกมีสมมาตรน้อยลง อย่างไรก็ตามในกรณีที่ศักย์ถูกเปลี่ยนแปลงไปเล็กน้อย ค่าพลังงานดังกล่าวยังคงมีค่าค่อนข้างมากเมื่ออิเล็กตรอนมีจำนวนเท่ากับ 2, 6 และ 12 ตัว นอกจากนี้ยังพบว่าเราสามารถอธิบายการจัดเรียงอิเล็กตรอนสปินด้วยกฎของฮุนได้เช่นเดียวกับอะตอม ผลการคำนวณที่ได้สอดคล้องกับผลการทดลองเป็นอย่างดี

ภาควิชา ฟิสิกส์ ลายมือชื่อนิสิต.....
สาขาวิชา ฟิสิกส์ ลายมือชื่ออาจารย์ที่ปรึกษา.....
ปีการศึกษา 2545

4272225023 : MAJOR PHYSICS

KEY WORD: SPIN-DENSITY FUNCTIONAL THOERY/ ELECTRONIC STRUCTRUCTURES / QUANTUM DOTS / EXCHANGE-CORRELATION ENERGY

KHATTIYA CHALAPAT : APPLICATION OF DENSITY FUNCTIONAL THEORY FOR A CIRCULAR QUANTUM DOT. THESIS ADVISOR : ASSOC. PROF. WICHIT SRITRAKOOL, Ph.D., 90 pp. ISBN 974-17-2892-1.

The objective of the thesis was to study the ground-state electronic structures of N-electron quantum dots. Calculations based on the spin-density-functional theory have been performed in real space within the local spin-density approximation. The recently proposed analytic representation of the exchange-correlation energy functional of Attaccalite *et al* was used instead of the most used form of Tanatar and Cepeley. The effect of the confining potential and the electron-electron interaction on the electronic structures were examined. For Harmonic confinement, the addition energy spectra obtained shows a clear shell structure as a function of N corresponding to the unusually large peaks at N = 2, 6, 12, and the smaller peaks at N = 4, and 9. The geometry deformation of a circular quantum dot was studied by varying the geometry parameter of anisotropic parabolic confining potential. The calculated results show that there still exists the shell structure corresponding to N = 2, 6 and 12 for the slightly deformed circular quantum dot. Shell-filling and spin configuration are found to determined mostly by Hund's rule. These findings are in very good agreement with previously observed experimental results.

Department Physics Student's signature.....

Field of study Physics Advisor's signature.....

Academic year 2002

Acknowledgements

The research described in this thesis was supported financially by a GSCU (Graduate School of Chulalongkorn University) studentship, and it is a great pleasure to be able to thank some of the people who have helped me in various ways.

First and foremost, I wish to express my deep gratitude to my supervisor, Assoc. Prof. Dr. Wichit Sritrakool for his advice, guidance, and encouragement throughout this work.

I would also like to thank Mr. Alongkorn Katwilart and Mr. Supitch Khemmani for many stimulating discussions and helpful comments. Warm thanks to Mr. Wattana Lim, Miss Suphatra Adulrattananuwat, Miss Orapin Niamploy and everyone at FTS for sharing and supporting all the time I have been there. Special thanks to Miss Piyanate Chuychai for supporting and helping me preparing the nice figures, without those this thesis would not have been completed. At last, but by no means least, a big Thank you to my family and all friends both in Thailand and Germany for their love and support.

Contents

Contents (continued)

List of Figures

List of Figures (continued)

List of Tables

Chapter 1

Introduction

Quantum dots (QDs) are structures that confine electrons three dimensionally in small space. The dimensions of the dot structures are of the order of an electron wavelength which is typically between 1 nm to 100 nm across. Scientists and engineers are interested in QDs for technical applications, and also as systems to test our understanding of quantum theory. Some applications include lasers, transistors, solar cells, and quantum computing devices. The physics of quantum dots shows many parallels with the behavior of atomic systems.

In atomic systems, electrons are confined by the attractive spherical symmetric potential. From quantum theory, this electrons are allowed to exist only with certain discrete energies corresponding to the 1s, 2s, 2p, 3s, ... orbital. Stability of the electronic system will occur when a shell is fully occupied such as in the nobel gas atoms. In the mid-shell levels, electrons normally keep spins parallel according to Hund's rules.

As in an atom, the energy levels in quantum dots become quantized due to the confinement of electrons. An experimental result reported by Tarucha *et al* (1996) shows that at zero magnetic field, the energy needed to add electrons to a circular QD reveals a clear shell structure of 2D harmonic potential [1]. The addition energy was unusually large when the electron number coincides with 2, 6, and 12. In addition, they also applied tunable magnetic fields to the dots and found that the spin filling order could be explained in terms of Hund's

rules. Experimental results on quantum dots of rectangular shapes have also been observed by Austing *et al* (1999) [2].

Motivated by the experimental work, Ezaki, Mori and Hamaguchi (1997) calculated electronic structures of quantum dots by numerically diagonalising the N-electron Hamiltonian (N up to 11) using Slater determinants formed from single-electron eigenfunction [3]. Since, the exact diagonalization is limited to a small number of particles, other well-established methods are needed to study quantum dots with a larger number of electrons. Recently, there have been a number of techniques used to calculate the electronic structure of a quantum dot, for example, Hartree-Fock approximation [4], Quantum Monte Carlo techniques [5], and Density-Functional Approaches [6],[7],[8].

Using spin-density-functional theory (SDFT), Koskinen *et al* (1997) calculated the ground-state electronic structures of circular parabolic quantum dots [6]. To avoid symmetry restrictions, they expanded the wave function in a plane-wave basis. Independently, Lee *et al* (1998) also studied 3D parabolic quantum dots by using a real space method based on spin-denisty-functional theory [8] up to N=12. Another different approach was also proposed by Hirose and Wingreen (1999)[7]. They studied the electronic states of a 2D parabolic quantum dot with up to N=58 electrons by expanding the eigenstates of the Kohn-Sham equation in single-electron basis known as Fock-Darwin representation [1]. All of the above spin-density-functional approaches applied to quantum dots were implemented by using the local-spin-density approximation (LSDA). Within LSDA, the exchange-correlation energy functional are taken to be functions of the local spin densities, which are defined by the requirement that the approximation be exact for the

[1]The case of a single electron in an isotropic 2D harmonic oscillator was solved independently by Fock (1928) and Darwin (1930) (see ref. [9], [10]).

homogeneous electron gas. The most used form of the exchange-correlation functional is the parametrized form of Tanatar and Ceperley which based on diffusion Quantum Monte Carlo (DMC) data at spin polarization $\zeta = 0$ and $\zeta = 1$ [11].

Recently, Attaccalite *et al* (2002) have presented new diffusion Quantum Monte Carlo simulations for a wide range of electron densities r_s and spin polarizations ζ[12]. This direct DMC calculation of ζ dependence is new and provides a reliable basis for building an LSD energy functional for 2D systems. Note that this new analytic representation is an extension to the most used parametrized form of Tanatar and Ceperly.

The aim of this thesis was to study the ground-state electronic structures of quantum dots. The calculations have been performed in real space by using a method based on spin-density functional theory. The new analytic representation of the exchange-correlation energy has been used instead of the most used form of Tanatar and Ceperley. The effects of the confining potential and the electron-electron interaction on the electronic structures were also discussed.

Chapter 2

Density-Functional Theory

In this chapter, we will introduce the principles of density-functional theory which have been known as a powerful approach to the quantum many-body problem. The introduction is given briefly in Sec 2.1. Some basic concepts in the path of the Schrödinger equation and the multiparticle wavefunctions are presented in Sec 2.2. The Hohenberg-Kohn variational principle, where the electron density $n(r)$ is the variational variable, is described in Sec. 2.3. Then, in Sec 2.4, the Kohn-Sham scheme, which was introduced in 1965 as a way to combine wavefunction and density approach, is presented. The extensions of the Kohn-Sham formalism to spin-polarised systems are given in Sec 2.5. Finally, in the last section, a brief discussion of the approximations for the exchange-correlation energy ($E_{xc}[n(r)]$) involved in the Kohn-Sham scheme is presented.

2.1 Introduction

For more than seven decades, after Schrödinger [13] proposed his wave equation in 1926, quantum systems have been considered as being described by state vectors in Hilbert space (wavefunctions in coordinate or momentum space) and observables by Hermitian operators. Principally, Schrödinger equation contains all information about the quantum systems such as atoms, molecules, and solids which comprise of electrons and nuclei. However, when one deals with realistic quantum many-body systems, the equations may be far too complex to allow

solution. In such cases, one must introduce an approximation method to solve the problem. Most of the methods are essentially based upon the variational principle. In this approach one guesses the form of the wavefunction with a set of parameters. The parameters are then varied to minimize the expectation value of the observables, particularly the energy of the system. As one knows, this is an extremely powerful approach, but it depends for its success upon a good parametric description of the problem in the first instance. That is, the better the form of wavefunction we take, the better results we will get from the variational approach.

The Hartree-Fock (1930, [14]) and Hartree (1928, [15]) methods are examples of formalism which can be derived from the variational principle [2]. The difference between them is the form of the trial wavefunction. The Hartree-Fock antisymmetric wavefunction (determinantal wavefunction) allows one to describe the exchange interaction, while the Hartree product wavefunction does not. However, another piece of Physics, called *correlation effects*, are still ignored in the Hartree-Fock formalism. These effects are small compared to the exchange effects in the systems like atoms or molecules, but will be much more significant in solid. To improve the approximation behind the Hartree-Fock method, a better approach should be introduced. The fact that the Hartree-Fock wavefunction is just a single configuration (Slater determinant) wave function leads us to an approach known as *configuration interaction* (CI). In CI method, the many-body wavefunction is described by the linear combination of single configurations (single determinantal functions). This leads, in principle, to the exact wavefunction

[2]From, the assumption of no correlations, the Hartree-Fock equation can also be derived, without recourse to the variational method, by assuming that the reduced density matrices of second- and third-order are particular functionals of the electron density or the first-order reduced density matrix [16].

in which all possible combinations have to be taken into account. The increase in the number of configurations or the dimension of the Hilbert space with increasing electron number means that only systems with a limited number of electrons can be calculated with high accuracy.

A different approach was taken by Thomas [17] and Fermi [18] in 1927-28. They proposed a scheme based on the electron density $n(r)$. The Thomas-Fermi scheme assumed that the motions of the electrons are uncorrelated and the corresponding kinetic energy can be described by a local approximation based on the results for free electrons [19]. The extensions of this scheme was suggested by Dirac (1930) who proposed that this scheme could be improved by including the exchange energy of a free electron gas. His work related the Hartree-Fock theory and the Thomas-Fermi model. The Thomas-Fermi-Dirac method was a true density functional method in which the system was characterized completely by the electron density $n(r)$. However, they did not demonstrate that ground-state properties, particularly the total energy E, could be related in a rigorous way to the density distribution. The theoretical justification for this scheme was proposed by Hohenberg and Kohn [20] in 1964. The formalism is, in principle, exact, and the Thomas-Fermi equation can be derived from it as an approximation. Its application to the total energy calculation is done in the context of the variational principle.

2.2 Basic Concepts

The Schrödinger equation

The electrons in a molecule or a solid interact strongly both with the ions and with each other. The challenge of modern electronic structure theory is to

go beyond the independent electron approximation. So far, the foundation of the theory is the nonrelativistic Schrödinger equation. For an isolated N-electron system in the Born-Oppenheimer approximation, this is given by

$$\widehat{H}\,|\Psi\rangle = E\,|\Psi\rangle \tag{2.1}$$

where $|\Psi\rangle$ called a state vector or state ket, represents quantum states of the N-electron system and $\widehat{H}$ is the Hamiltonian operator,

$$\widehat{H} = -\sum_{i=1}^{N}\frac{1}{2}\nabla_i^2 + \frac{1}{2}\sum_{i\neq j}^{N}\frac{1}{|\mathbf{r}_i-\mathbf{r}_j|} - \sum_{i,l}^{N}\frac{Z_l}{|\mathbf{r}_i-\mathbf{R}_l|} \tag{2.2}$$

where $\mathbf{r}_i$ are the positions of the electron, and $\mathbf{R}_l$ are the positions of the nuclei.

The N-electron wave function in coordinate space is related to the state vector in Hilbert space by

$$\Psi(\mathbf{x}_1,\mathbf{x}_2,...,\mathbf{x}_N) = \langle \mathbf{x}_1,\mathbf{x}_2,...\mathbf{x}_N|\Psi\rangle\,. \tag{2.3}$$

The wave function Ψ depends on both the positions and spins of the N electrons. $\mathbf{x}\equiv(\mathbf{r},s)$. The Pauli exclusion principle requires that

$$P_{ij}\Psi = -\Psi \tag{2.4}$$

where P_{ij} permutes the space and spin coordinates of electrons i and j. In other words, the wavefunction Ψ is antisymmetric.

The expectation value of an observable Ω in the quantum state Ψ is given by the formular

$$\langle\Omega\rangle = \langle\Psi|\,\widehat{\Omega}\,|\Psi\rangle \tag{2.5}$$

where

$$\langle\Psi|\,\widehat{\Omega}\,|\Psi\rangle = \int \prod_{i=1}^{N} d\mathbf{x}_i \Psi^*(\mathbf{x}_1, \mathbf{x}_2, ..., \mathbf{x}_N)\ \widehat{\Omega}\Psi\left(\mathbf{x}_1, \mathbf{x}_2, ..., \mathbf{x}_N\right) \tag{2.6}$$

Rayleigh-Ritz variational principle

When a system is in the state $|\Psi\rangle$ which may or may not satisfy (2.1) the expectation value of the energy is

$$E\left[\Psi\right] = \langle\Psi\,|H|\,\Psi\rangle\,. \tag{2.7}$$

The expectation value $\langle\Psi\,|H|\,\Psi\rangle$ is a functional; given Ψ one gets a number from this prescription.

The Rayleigh-Ritz variational principle states that the expectation value of E in any state is greater than the ground-state energy,

$$E\left[\Psi\right] \geq E_0. \tag{2.8}$$

That is, the energy computed from a guessed Ψ is an upper bound to the ground-state energy E_0. The following is formal proof of the variational principle (2.8):

Expand the state $|\Psi\rangle$ in terms of the normalized eigenstates of $\widehat{H}$:

$$|\Psi\rangle = \sum_n a_n\,|\Psi_n\rangle\,, \tag{2.9}$$

the expectation value of the energy becomes

$$E[\Psi] = \frac{\sum_{nm} \langle \Psi_n | \widehat{H} | \Psi_m \rangle a_n^* a_m}{\sum_n |a_n|^2} \tag{2.10}$$

$$= \frac{\sum_n E_n |a_n|^2}{\sum_n |a_n|^2}. \tag{2.11}$$

Since, E_n is always greater than or equal to E_0, we obtain

$$\sum_n E_n |a_n|^2 \geq E_0 \sum_n |a_n|^2 \tag{2.12}$$

Thus,

$$E[\Psi] \geq E_0. \tag{2.13}$$

To illustrate this principle, we will show how the Schrödinger equation (2.1) is derived in this context. At the extremum, the energy functional $E[\Psi]$ is stationary with respect to the variation of Ψ:

$$\delta E[\Psi] = 0. \tag{2.14}$$

That is,

$$0 = \delta \left[\langle \Psi | \widehat{H} | \Psi \rangle - E \langle \Psi | \Psi \rangle \right] \tag{2.15}$$

$$= \langle \delta\Psi | \widehat{H} - E | \Psi \rangle + \langle \Psi | \widehat{H} - E | \delta\Psi \rangle .$$

Since $\widehat{H}$ is a Hermitian operator; $H = H^\dagger$, the condition (2.15) will be satisfied if

$$(\widehat{H} - E) | \Psi \rangle = 0.$$

This means when (2.14) is satisfied, so is (2.1).

Mutiparticle wavefunction-an exponential wall limiting the number of particles

Traditional multiparticle wavefunction methods when applied to systems of many particles encounter an exponential wall [21]. This conclusion can be understood easily as follow. Let p be the number of parameters per variable needed for the desired accuracy. For example, assume that the wavefunction we are looking for is confined in an one-dimension region L. If we divide this region into equidistant mesh points z_i each separated in real space by a distance Δz, the number of parameters p needed will be equal to $L/\Delta z + 1$. Similarly, let us consider the multiparticle wavefunction $\Psi(r_1, ..., r_N)$, the number of variables of Ψ is 3N if we ignore symmetries and spin, which will not affect our general conclusions. We can easily see that the number of parameters required for this accuracy is

$$M = p^{3N}. \tag{2.16}$$

The energy needs to be minimized in the space of these parameters. Call $\overline{M}$ the maximum value which is capable of being done by the available computer software and hardware; and $\overline{N}$ the corresponding maximum number of electrons. Then, from Eq. 2.16 we get

$$\overline{N} = \frac{1}{3}\frac{\ln \overline{M}}{\ln p}. \tag{2.17}$$

Let us optimistically take $\overline{M} \approx 10^{10}$ and $p = 10$. This gives the shocking result

$$\overline{N} = \frac{1}{3}\frac{\ln 10^{10}}{\ln 10} = \frac{10}{3} \longrightarrow 3. \tag{2.18}$$

In practice, one can do better than this. But the exponential in 2.16 still represents a wall limiting $\overline{N}$. This can lead us to the conclusion that traditional wavefunction methods, which provide the required physical and chemical accuracy, are generally limited to systems with a small total number of active electrons.

Electron density

Unlike the wavefunction, electron density $n(r)$ is an observable quantity depending only on coordinates in real space. One can obtain the electron density for electron ith by integrating the total probability density $|\Psi|^2$ over all the coordinates of the other $n-1$ electrons:

$$n_i(\mathbf{x}_i) = \int \prod_{j \neq i}^{N} d\mathbf{x}_j \left|\Psi\left(\mathbf{x}_1, \mathbf{x}_2, ..., \mathbf{x}_N\right)\right|^2 \tag{2.19}$$

and the total electron density $n(\mathbf{x})$ for the presence of all electrons is just the sum of all $n_i(\mathbf{x})$

$$n(\mathbf{x}) = \sum_{i=1}^{N} n_i(\mathbf{x}). \tag{2.20}$$

Since electrons are indistinguishable, all $n_i(\mathbf{x})$ must be the same. Therefore, we can rewrite (2.20) as follows:

$$n(\mathbf{x}) = N \int \prod_{i=2}^{N} d\mathbf{x}_i \left|\Psi\left(\mathbf{x}, \mathbf{x}_2, ..., \mathbf{x}_N\right)\right|^2. \tag{2.21}$$

In many cases, operators of interest do not involve spin coordinates. This makes further reduction of the electron density in (2.21) by summation over the spin coordinates.

$$n(\mathbf{r}) = N \int \prod_{i=1}^{N} d\mathbf{x}_i ds \left|\Psi\left(\mathbf{r},s,\mathbf{x}_2,...,\mathbf{x}_N\right)\right|^2 . \tag{2.22}$$

Now, the relation between the electron density and the external potential of which the electrons are moving under the influence will be derived. Consider the external potential energy operators $\widehat{V}$ of the form:

$$\widehat{V} = \sum_{i=1}^{N} v(\mathbf{r}_i). \tag{2.23}$$

The contribution of $\widehat{V}$ to the total energy is

$$\langle\Psi|\,\widehat{V}\,|\Psi\rangle = \sum_{i=1}^{N} \int \prod_{i=1}^{N} d\mathbf{x}_i \Psi^*(\mathbf{x}_1,...,\mathbf{x}_N) v(r_i) \Psi(\mathbf{x}_1,...,\mathbf{x}_N). \tag{2.24}$$

Using the definition of $n_i(\mathbf{x}_i)$ in Eq. (2.19), and the fact that the operator $v(r_i)$ is multiplicative; i.e. has no operator terms like differential operator, and dependent only on the coordinates of electron ith:

$$\langle\Psi|\,\widehat{V}\,|\Psi\rangle = \sum_{i=1}^{N} \int v(\mathbf{r}_i) n_i(\mathbf{x}_i) d\mathbf{x}_i. \tag{2.25}$$

Similarly, by using (2.22), the above equation can be rewritten as

$$\langle\Psi|\,\widehat{V}\,|\Psi\rangle = \int v(\mathbf{r}) n(\mathbf{r}) d^3r. \tag{2.26}$$

Eq. (2.26) leads us to the conclusion that an external potential energy is a functional of electron density. The result is general; the expectation value of any symmetrical sum of one-electron operators is the integral of any one of them with the electron density. We can see that without the multiplicative property one can not rearrange the integrand into the final form. So, it seems to be impossible

to evaluate the expectation value of any observables with only a knowledge of the electron density. However, the Density-Functional theory implies that it is principally possible.

2.3 The Hohenberg-Kohn Theorem

The initial work on Density-Functional Theory (DFT) was reported in 1964 by P. Kohenberg and W. Kohn [20] . They proved that the ground-state density $n(r)$ of a bound system of interacting electrons in some external potential $\widehat{V}$ determines this potential uniquely. More specifically, $n(r)$ determines implicitly all properties derived from $\widehat{H}$ (Eq. 2.30).

Before Hohenberg and Kohn published their landmark paper[20], there had existed the Thomas-Fermi (Thomas [17], 1927; Fermi [18], 1928) theory which considered interacting electrons moving in an external potential $v(r)$, and provided a one-to-one relation between $v(r)$ and the density $n(r)$:

$$n(\mathbf{r}) = \gamma[\mu - v_{eff}(\mathbf{r})]^{3/2} \tag{2.27}$$

in which

$$v_{eff}(\mathbf{r}) \equiv v(\mathbf{r}) + \int \frac{n(\mathbf{r}')}{|\mathbf{r} - \mathbf{r}'|} d^3r \tag{2.28}$$

where μ is the r-independent chemical potential, and $\gamma = \frac{1}{3\pi^2}\left(\frac{2m}{\hbar^2}\right)^{3/2}$. Eq. 2.27 is based on the expression

$$n = \gamma(\mu - v)^{3/2} \tag{2.29}$$

for the density of a uniform electron gas in constant external potential.

The TF theory showed how to roughly express physical properties in terms of $n(r)$. But the use of electron density as a fundamental description of the system was based on intuition rather than hard proof that this can be done. However, the situation changed with the publication of the landmark paper by Hohenberg and Kohn. They provided the fundamental theorems showing that for ground states the TF theory may be regarded as an approximation to an exact theory, the *Density-Functional Theory*. Hohenberg and Kohn have shown that it is possible, in principle, to completely describe the electronic structure in terms of $n(r)$.

The basic lemma of HK.

The ground-state density $n(r)$ of a bound system of interacting electrons in some external potential $v(r)$ determines this potential uniquely [20] ,[21].

Remark: 1. The term uniquely means: up to an uninteresting additive constant. 2. In case of a degenerate ground state, the lemma refers to any ground-state density $n(r)$.

This lemma means there is a one-to-one correspondence between the ground state density of the many-fermion system and the external potential acting upon it. The proof of this is very simple. The N-electron systems under consideration are characterized by a non-relativistic Hamiltonian

$$\widehat{H} = \widehat{T} + \widehat{U} + \widehat{V} \tag{2.30}$$

where $\widehat{T}$ is the kinetic energy operator, $\widehat{U}$ is the e-e interaction energy operator, and $\widehat{V}$ is the external potential energy operator:

$$\widehat{V} = \sum_{i=1}^{N} v(\mathbf{r}_i). \tag{2.31}$$

For a molecule or solid, $v(\mathbf{r}_i)$ is the external potential acting on electron i, due to nuclei.

Let $n(\mathbf{r})$ be the nondegenerate ground-state density in the external potential $v_1(\mathbf{r})$, corresponding to the nondegenerate ground state Ψ_1 and the energy E. Then,

$$\begin{aligned} E_1 &= \langle \Psi_1 | \, \widehat{H}_1 \, | \Psi_1 \rangle \\ &= \langle \Psi_1 | \, \widehat{T} + \widehat{U} \, | \Psi_1 \rangle + \int v_1(\mathbf{r}) n(\mathbf{r}) d^3 r. \end{aligned} \tag{2.32}$$

Assume $v_2(\mathbf{r})$, not equal $v_1(\mathbf{r})$+constant, to be another potential with the ground state Ψ_2 giving rise to the same ground-state density $n(\mathbf{r})$. ($\Psi_1 \neq \Psi_2$ since they satisfy different Schrodinger equations.) Then,

$$\begin{aligned} E_2 &= \langle \Psi_2 | \, \widehat{H}_2 \, | \Psi_2 \rangle \\ &= \langle \Psi_2 | \, \widehat{T} + \widehat{U} \, | \Psi_2 \rangle + \int v_2(\mathbf{r}) n(\mathbf{r}) d^3 r. \end{aligned} \tag{2.33}$$

Since Ψ_1 is assumed to be nondegerate, the Rayleigh-Ritz minimal principle gives the inequality:

$$\begin{aligned} \langle \Psi_1 | \, \widehat{H}_1 \, | \Psi_1 \rangle &< \langle \Psi_2 | \, \widehat{H}_1 \, | \Psi_2 \rangle \\ E_1 &< \langle \Psi_2 | \, \widehat{H}_2 \, | \Psi_2 \rangle + \langle \Psi_2 | \, \widehat{H}_1 - \widehat{H}_2 \, | \Psi_2 \rangle \\ E_1 &< E_2 + \int \left(v_1(\mathbf{r}) - v_2(\mathbf{r}) \right) n(\mathbf{r}) d^3 r. \end{aligned} \tag{2.34}$$

Similarly,

$$\begin{aligned}
\langle\Psi_2|\,\widehat{H}_2\,|\Psi_2\rangle &\leq \langle\Psi_1|\,\widehat{H}_2\,|\Psi_1\rangle \\
E_2 &\leq \langle\Psi_1|\,\widehat{H}_1\,|\Psi_1\rangle + \langle\Psi_1|\,\widehat{H}_2 - \widehat{H}_1\,|\Psi_1\rangle \\
E_2 &\leq E_1 + \int \left(v_2(\mathbf{r}) - v_1(\mathbf{r})\right) n(\mathbf{r}) d^3r, \qquad (2.35)
\end{aligned}$$

where we use $\leq$ since the non-degeneracy of Ψ_2 was not assumed. Adding Eqs. (2.34) and (2.35) leads to the contradiction

$$E_1 + E_2 < E_1 + E_2. \qquad (2.36)$$

We conclude that the assumption of the existence of a second potential $v_2(\mathbf{r})$ which is unequal to $v_1(\mathbf{r})$+constant and gives the same $n(\mathbf{r})$ must be wrong. The lemma is thus proved for nondegenerate ground state. In the case of degenerate-ground state, the proof can easily extended, see Ref. [22], [23].

It is clear now that the electron density determines the external potential $\widehat{V}$ of which the system is under the influence. Hence, the value of E is fixed by $n(\mathbf{r})$ to within a constant, i.e., the total ground-state energy is a functional of electron density $n(\mathbf{r})$:

$$\begin{aligned}
\langle\Psi|\,(\widehat{T} + \widehat{U} + \widehat{V})\,|\Psi\rangle &= E\left[n\left(\mathbf{r}\right)\right] \\
&= F\left[n\left(\mathbf{r}\right)\right] + \int v(\mathbf{r}) n(\mathbf{r}) d^3r, \qquad (2.37)
\end{aligned}$$

where

$$F\left[n\left(\mathbf{r}\right)\right] \equiv \langle\Psi|\,(\widehat{T} + \widehat{U})\,|\Psi\rangle\,. \qquad (2.38)$$

The functional $F[n(\mathbf{r})]$ is universal in the sense that its form does not depend on the external potential. So, once we have an explicit form of $F[n(\mathbf{r})]$ we can apply to any system under consideration.

It should be emphasized that the density $n(\mathbf{r})$ in the Hohenberg-Kohn theorems must be in the set of v-representable (VB) densities. This means $n(\mathbf{r})$ must be the density associated with the ground-state wavefunction of a Hamiltonian of the form (2.30) with some external potential $v(\mathbf{r})$. The Hohenberg-Kohn basic lemma can be restated as follows: The v-representable ground-state density $n(r)$ of interacting electrons in some external potential $v(r)$ determines this potential uniquely.

The HK variational principle

For all v-representable trial density $\widetilde{n}(\mathbf{r})$ *such that* $\widetilde{n}(\mathbf{r}) \geq 0$, *and* $\int \widetilde{n}(\mathbf{r}) d^3r = N$,

$$E[\widetilde{n}(\mathbf{r})] \equiv F[\widetilde{n}(\mathbf{r})] + \int v(\mathbf{r})\widetilde{n}(\mathbf{r}) d^3r \geq E[n_0(\mathbf{r})], \tag{2.39}$$

where $E[n_0(\mathbf{r})]$ *is the ground-state energy of the Hamiltonian with* $v(\mathbf{r})$ *as an external potential, and* $n_0(\mathbf{r})$ *its ground-state density.*

That means the total energy calculated from a trial density $\widetilde{n}(\mathbf{r})$ can not be lower than the true ground-state energy. The variational principle can be easily proved, since each trial density $\widetilde{n}(\mathbf{r})$ is a ground-state density corresponding to some external potential. As long as each trial density defines a Hamiltonian, one can derive the corresponding ground-state $\widetilde{\Psi}$.

$$\widetilde{n}(\mathbf{r}) \rightarrow \widetilde{\Psi}.$$

According to the Rayleigh-Ritz variational principle, we obtain

$$\left\langle \widetilde{\Psi} \right| \widehat{H} \left| \widetilde{\Psi} \right\rangle \geq \langle \Psi_0 | \widehat{H} | \Psi_0 \rangle \tag{2.40}$$

$$E\left[\widetilde{n}\left(\mathbf{r}\right)\right] \geq E\left[n_0\left(\mathbf{r}\right)\right], \tag{2.41}$$

where $n_0\left(\mathbf{r}\right)$ is the real ground-state density of the system of interest.

The ground-state energy and density can be obtained by using the method of Lagrange multiplier. The electron density is varied within the constraint

$$\int \widetilde{n}\left(\mathbf{r}\right) d^3r = N, \tag{2.42}$$

and the energy is stationary for small variations $\delta\widetilde{n}\left(\mathbf{r}\right)$ around the exact ground density $n_0\left(\mathbf{r}\right)$,

$$\delta E\left[\widetilde{n}\left(\mathbf{r}\right)\right] = \int \left[v\left(\mathbf{r}\right) + \frac{\delta}{\delta\widetilde{n}\left(\mathbf{r}\right)} F\left[\widetilde{n}\left(\mathbf{r}\right)\right]|_{\widetilde{n}=n_0} - \mu\right] \delta\widetilde{n}\left(\mathbf{r}\right) d^3r = 0, \tag{2.43}$$

which leads to

$$\mu = v\left(\mathbf{r}\right) + \frac{\delta F\left[n\left(\mathbf{r}\right)\right]}{\delta n\left(\mathbf{r}\right)}. \tag{2.44}$$

The quantities μ is the undertermined Lagrange multiplier. If we knew the form of $F\left[n\left(\mathbf{r}\right)\right]$, (2.44) would be an exact equation for the ground-state density.

The HK variational principle is verified only for v-representable density. So, one has to be sure that each trial density belongs to the domain of v-representable densities. The first extension of HK formalism to non-v-representable density was proposed by Levy [24] (1979) and the further investigation by Lieb [25] (1982) and Levy [26] (1982).

The Levy-Lieb constrained-search formulation

Let us recall the Rayleigh-Ritz variational principle

$$\left\langle \widetilde{\Psi} \right| \widehat{H} \left| \widetilde{\Psi} \right\rangle \geq \langle \Psi_0 | \, \widehat{H} \, | \Psi_0 \rangle \, .$$

We know that every trial wavefunction $\widetilde{\Psi}$ corresponds to a trial density $\widetilde{n}\left(\mathbf{r}\right)$, but there exists an infinite number of antisymmetric wavefunctions that give the same density. So, one may carry out the minimization in two steps: First fix a trial density $\widetilde{n}\left(\mathbf{r}\right)$ and search over the set of trial wavefunctions which corresponds to this density $\widetilde{n}\left(\mathbf{r}\right)$. The constrained energy mimimum with fixed $\widetilde{n}\left(\mathbf{r}\right)$ is defined as

$$\begin{aligned} E\left[\widetilde{n}\left(\mathbf{r}\right)\right] &\equiv \min_{\widetilde{\Psi}\rightarrow\widetilde{n}(\mathbf{r})} \left\langle \widetilde{\Psi} \right| \widehat{H} \left| \widetilde{\Psi} \right\rangle \\ &= \int v(\mathbf{r})\widetilde{n}(\mathbf{r})d^3r + F_{LL}\left[\widetilde{n}\left(\mathbf{r}\right)\right], \end{aligned} \tag{2.45}$$

where

$$F_{LL}\left[\widetilde{n}\left(\mathbf{r}\right)\right] \equiv \min_{\widetilde{\Psi}\rightarrow\widetilde{n}(\mathbf{r})} \left\langle \widetilde{\Psi} \right| \widehat{T} + \widehat{U} \left| \widetilde{\Psi} \right\rangle . \tag{2.46}$$

In the second step, minimize (2.45) over all $\widetilde{n}\left(\mathbf{r}\right)$,

$$E\left[\widetilde{n}\left(\mathbf{r}\right)\right] \equiv \min_{\widetilde{n}} \left[\int v(\mathbf{r})\widetilde{n}(\mathbf{r})d^3r + F_{LL}\left[\widetilde{n}\left(\mathbf{r}\right)\right] \right]. \tag{2.47}$$

Noting that, in this constrained search, trial densities $\widetilde{n}\left(\mathbf{r}\right)$ are v-representable, since they corresponds to some antisymmetric wavefunctions.

The Thomas-Fermi theory

The variational principle may be considered as the exactification of Thomas-Fermi theory. Consequently, one could easily rederive the Thomas-Fermi (2.27) equation by taking

$$F\left[n\left(\mathbf{r}\right)\right] = T_{TF}\left[n\left(\mathbf{r}\right)\right] + U_{es}\left[n\left(\mathbf{r}\right)\right]$$

where

$$T_{TF}[n\left(\mathbf{r}\right)] = C_F \int n^{5/3}\left(\mathbf{r}\right) d^3r, \quad \text{where } C_F = \frac{3}{10}\frac{\hbar^2}{m}(3\pi^2)^{2/3} \tag{2.48}$$

and

$$U_{es}\left[n\left(\mathbf{r}\right)\right] = \frac{1}{2}\int \frac{n\left(\mathbf{r}\right) n\left(\mathbf{r}'\right)}{|\mathbf{r}-\mathbf{r}'|} d^3r d^3r'. \tag{2.49}$$

The expression of $U_{es}\left[n\left(\mathbf{r}\right)\right]$ is the classical (mean-field) approximation.

2.4 The Basic Kohn-Sham Scheme

Kohn and Sham (1965) introduced the idea of an auxiliary noninteracting-electron system such that the corresponding electron density equals to the density of the real interacting-electron system [27]. The idea enabled them to combine the Hohenberg-Kohn variational principle with traditional wavefunction methods. In this section, we present the Kohn-Sham scheme in the situation where the spin degrees of freedom are neglected. The more difficult situation will be presented in the following sections.

Consider an interacting-electron system described by the Hamiltonian as in Eq. (2.30)

$$\widehat{H} = \widehat{T} + \widehat{U} + \widehat{V}.$$

According to the theorem of Hohenberg and Kohn, there exists the energy functional (2.37)

$$E[n(\mathbf{r})] = F[n(\mathbf{r})] + \int v(\mathbf{r}) n(\mathbf{r}) d^3r$$

where the universal functional $F[n(\mathbf{r})]$ contains both kinetic and interaction energy.

Kohn and Sham proposed an approximation of $F[n(\mathbf{r})]$, which after applying the variational principle to the new energy functional, yields a self-consistent single-particle Schrödinger equation with a local effective potential $v_{eff}(\mathbf{r})$. The scheme is analogous to the Hartree method but contains the part of the exchange and correlation effects.

The HK universal functional $F[n(\mathbf{r})]$ was seperated as follows:

$$F[n(\mathbf{r})] \equiv T_s[n(\mathbf{r})] + \frac{1}{2}\int \frac{n(\mathbf{r})\, n(\mathbf{r}')}{|\mathbf{r} - \mathbf{r}'|} d^3r d^3r' + E_{xc}[n(\mathbf{r})], \tag{2.50}$$

where $T_s[n(\mathbf{r})]$ is the kinetic energy of electrons in a system which has the same density $n(\mathbf{r})$ as the real system, but in which there is no electron-electron interactions. $E_{xc}[n(\mathbf{r})]$ is called exchange-correlation energy (because of its origin in the correlated motion of electrons and the quantum effects implied from the Pauli exclusion principle). It has to be stressed that $E_{xc}[n(\mathbf{r})]$ also contains the correction for self-interaction introduced by the classical electrostatic potential. Eq. (2.50) leads us to a new expression for the energy functional

$$E\left[n\left(\mathbf{r}\right)\right]=T_{s}\left[n\left(\mathbf{r}\right)\right]+\frac{1}{2}\int\frac{n\left(\mathbf{r}\right)n\left(\mathbf{r}'\right)}{\left|\mathbf{r}-\mathbf{r}'\right|}d^{3}rd^{3}r'+E_{xc}\left[n\left(\mathbf{r}\right)\right]+\int v(\mathbf{r})n(\mathbf{r})d^{3}r. \quad (2.51)$$

If we define the exchange-correlation potential as

$$v_{xc}\left(\mathbf{r};[n]\right)\equiv\frac{\delta E_{xc}\left[n\left(\mathbf{r}\right)\right]}{\delta n\left(\mathbf{r}\right)}, \quad (2.52)$$

the HK variational principle will lead us to the equation

$$\delta E\left[\widetilde{n}\left(\mathbf{r}\right)\right]=\int\left[\frac{\delta}{\delta\widetilde{n}\left(\mathbf{r}\right)}T_{s}\left[\widetilde{n}\left(\mathbf{r}\right)\right]|_{\widetilde{n}=n_{0}}+v_{eff}\left(\mathbf{r}\right)-\mu\right]\delta\widetilde{n}\left(\mathbf{r}\right)d^{3}r=0 \quad (2.53)$$

where we grouped all potential terms together into an effective potential:

$$v_{eff}\left(\mathbf{r}\right)\equiv v\left(\mathbf{r}\right)+\int\frac{n\left(\mathbf{r}\right)}{\left|\mathbf{r}-\mathbf{r}'\right|}d^{3}r+v_{xc}\left(\left[n\right];\mathbf{r}\right). \quad (2.54)$$

It should be stressed here that the seperation in Eq. (2.50) was the only approximation used for establishing the Kohn-Sham equations. This approximation is verified if the existence of an auxiliary system in which there is no electron-electron interactions, such that the corresponding ground-state density is equal to the ground-state density of the real interacting system, is assumed. (See Ref. [23] for further discussion.)

Now what one has to do is just solving the auxiliary problem to get the real ground-state density from which, according to the HK theorem, other properties of the real system may be calculated.

Kohn and Sham observed that Eq. (2.53) is identical to the equation for noninteracting electrons moving in the effective potential $v_{eff}\left(\mathbf{r}\right)$. Therefore, we can solve Eq. (2.53) by using the single-particle equation

$$\left[-\frac{1}{2}\nabla^2 + v_{eff}(\mathbf{r})\right]\varphi_i(\mathbf{r}) = \varepsilon_i\varphi_i(\mathbf{r}) \tag{2.55}$$

with

$$n(\mathbf{r}) = \sum_{i=1}^{N} |\varphi_i(\mathbf{r})|^2 . \tag{2.56}$$

The set of equations (2.54)-(2.56), are now called the Kohn-Sham equations. Since, the effective potential $v_{eff}(\mathbf{r})$ depends on the density, the whole equations have to be solved self-consistently: One begins with the assumed $n(\mathbf{r})$, constructs $v_{eff}(\mathbf{r})$ and finds a new $n(\mathbf{r})$ from (2.55) and (2.56). The ground-state energy is given by

$$E = \sum_{i=1}^{N} \varepsilon_i - \frac{1}{2}\int \frac{n(\mathbf{r})\, n(\mathbf{r}')}{|\mathbf{r}-\mathbf{r}'|} d^3r d^3r' - \int v_{xc}(\mathbf{r}) n(\mathbf{r}) d^3r + E_{xc}[n(\mathbf{r})] . \tag{2.57}$$

2.5 Spin-Density Functional Theory

The formal justification of the Spin-Density Functional Theory (SDFT) as an extension of the Hohenberg and Kohn formalism was firstly introduced simultaneously by von Barth and Hedin [28] and by Pant and Rajagopal [29] in 1972 (see also Rajagopal and Callaway [30], 1973). The SDFT is a necessary generalization for many-elecron systems in the presence of an external magnetic field.

In the presence of a magnetic field $\mathbf{B}(\mathbf{r})$ that interacts only with the electron spins, the Hamiltonian of the system can be written as

$$\widehat{H} = \widehat{T} + \widehat{U} + \widehat{V} + \widehat{E}_{mag}, \tag{2.58}$$

where $\widehat{T}$, $\widehat{U}$ and $\widehat{V}$ have been defined earlier in (2.30) and

$$\widehat{E}_{mag} = 2\mu_B \sum^{N} \mathbf{B}(\mathbf{r}) \cdot \mathbf{s}_i, \tag{2.59}$$

where $\mu_B = e\hbar/2m_e c$ is the Bohr-magneton, and $\mathbf{s}_i$ is the spin for electron ith. Here, for notational simplicity, we will consider the case where $B(\mathbf{r})$ have only a nonvanishing z-component

$$\mathbf{B}(\mathbf{r}) = (0, 0, B_Z(\mathbf{r})). \tag{2.60}$$

The ground-state energy is given by

$$\begin{aligned} E_0 &= \min_{\Psi} \langle \Psi | \widehat{H} | \Psi \rangle \\ &= \min_{n_\uparrow, n_\downarrow} \left[\min_{\widetilde{\Psi} \to \widetilde{n}_\uparrow, \widetilde{n}_\downarrow} \left\langle \widetilde{\Psi} \middle| \widehat{T} + \widehat{U} \middle| \widetilde{\Psi} \right\rangle + \int (v(\mathbf{r}) + \mu_B B_Z(\mathbf{r})) n_\uparrow(\mathbf{r}) d^3r \right. \\ &\qquad \left. + \int (v(\mathbf{r}) - \mu_B B_Z(\mathbf{r})) n_\downarrow(\mathbf{r}) d^3r \right] \\ &= \min_{n_\uparrow, n_\downarrow} \left[F[n_\uparrow, n_\downarrow] + \int (v(\mathbf{r}) + \mu_B B_Z(\mathbf{r})) n_\uparrow(\mathbf{r}) d^3r \right. \\ &\qquad \left. + \int (v(\mathbf{r}) - \mu_B B_Z(\mathbf{r})) n_\downarrow(\mathbf{r}) d^3r \right]. \end{aligned} \tag{2.61}$$

The last equality of (2.61) is the basis of the spin-density functional theory: $n_\uparrow$, and $n_\downarrow$ are all needed to describe the ground state of the many-electron system in the presence of a magnetic field $B_Z(\mathbf{r})$. However, $F[n_\uparrow, n_\downarrow]$ is unknown, and approximation is necessary for the theory to be implemented.

The Kohn-Sham method can now be introduced to handle the kinetic contribution to $F[n_\uparrow, n_\downarrow]$. In the manner of (2.50), define

$$F\left[n_{\uparrow}, n_{\downarrow}\right] = T_s\left[n_{\uparrow}, n_{\downarrow}\right] + \frac{1}{2}\int \frac{n\left(\mathbf{r}\right) n\left(\mathbf{r}'\right)}{\left|\mathbf{r}-\mathbf{r}'\right|} d^3r d^3r' + E_{xc}\left[n_{\uparrow}, n_{\downarrow}\right], \tag{2.62}$$

where $T_s\left[n_{\uparrow}, n_{\downarrow}\right]$ is the Kohn-Sham kinetic energy functional corresponding to a system of noninteracting electrons with density $n_{\uparrow}$, and $n_{\downarrow}$. Since, $T_s\left[n_{\uparrow}, n_{\downarrow}\right]$ can be expressed as a functional of one-electron wavefunctions $\varphi_i^{(\alpha)}(\mathbf{r})$, one can find the spin-related Kohn-Sham equations by the variation of the total energy functional with respect to $\varphi_i^{(\alpha)}(\mathbf{r})$, subject to normalization constraints, where α ($\uparrow$ or $\downarrow$) denotes the spin projection in the z-direction:

$$\int \left|\varphi_i^{(\alpha)}(\mathbf{r})\right|^2 d^3r = 1. \tag{2.63}$$

The resulting Kohn-Sham equations are

$$\left[-\frac{1}{2}\nabla^2 + v_{eff}^{(\alpha)}\left(\mathbf{r}\right)\right]\varphi_i^{(\alpha)}(\mathbf{r}) = \varepsilon_i^{(\alpha)}\varphi_i^{(\alpha)}(\mathbf{r}), \tag{2.64}$$

where the spin-dependent effective potentials are

$$v_{eff}^{\uparrow}\left(\mathbf{r}\right) = v\left(\mathbf{r}\right) + \mu_B B\left(\mathbf{r}\right) + \int \frac{n\left(\mathbf{r}\right)}{\left|\mathbf{r}-\mathbf{r}'\right|} d^3r + \frac{\delta E_{xc}\left[n_{\uparrow}, n_{\downarrow}\right]}{\delta n_{\uparrow}\left(\mathbf{r}\right)}$$

$$v_{eff}^{\downarrow}\left(\mathbf{r}\right) = v\left(\mathbf{r}\right) - \mu_B B\left(\mathbf{r}\right) + \int \frac{n\left(\mathbf{r}\right)}{\left|\mathbf{r}-\mathbf{r}'\right|} d^3r + \frac{\delta E_{xc}\left[n_{\uparrow}, n_{\downarrow}\right]}{\delta n_{\downarrow}\left(\mathbf{r}\right)} \tag{2.65}$$

and

$$n_{\sigma}\left(\mathbf{r}\right) = \sum_{i=1}^{N_{\sigma}} \left|\varphi_i^{(\sigma)}(\mathbf{r})\right|^2, \quad n\left(\mathbf{r}\right) = n_{\uparrow}\left(\mathbf{r}\right) + n_{\downarrow}\left(\mathbf{r}\right) \tag{2.66}$$

where

$$v_{xc}^{(\alpha)}\left(\mathbf{r};\left[n_{\uparrow},n_{\downarrow}\right]\right)\equiv\frac{\delta E_{xc}\left[n_{\uparrow},n_{\downarrow}\right]}{\delta n_{\sigma}\left(\mathbf{r}\right)}. \tag{2.67}$$

The states $\varphi_i^{(\alpha)}(\mathbf{r})$ are ordered so that the energies $\varepsilon_i^{(\alpha)}$ are non-decreasing. Now, similar to the expression in Eq. (2.57), the ground-state energy is given by

$$E_0=\sum_{i=1}^{\infty}\sum_{\sigma}\varepsilon_i^{(\sigma)}-\frac{1}{2}\int\int\frac{n\left(\mathbf{r}\right)n\left(\mathbf{r}'\right)}{\left|\mathbf{r}-\mathbf{r}'\right|}d^3r'd^3r-\sum_{\sigma}\int v_{xc}^{(\sigma)}\left(\left[n_{\uparrow},n_{\downarrow}\right];\mathbf{r}\right)n_{\sigma}\left(\mathbf{r}\right)d^3r+E_{xc}\left[n_{\uparrow},n_{\downarrow}\right]. \tag{2.68}$$

2.6 The Exchange-Correlation-Energy Functional

One can see from the definition in Eq. (2.50)

$$E_{xc}\left[n\left(\mathbf{r}\right)\right]\equiv F\left[n\left(\mathbf{r}\right)\right]-T_s\left[n\left(\mathbf{r}\right)\right]-\frac{1}{2}\int\frac{n\left(\mathbf{r}\right)n\left(\mathbf{r}'\right)}{\left|\mathbf{r}-\mathbf{r}'\right|}d^3rd^3r'$$

that $E_{xc}\left[n\left(\mathbf{r}\right)\right]$ includes the energy contributions from three parts: first, the non-classical part of electron-electron interaction energy. Second, correction from self-interaction introduced by the electrostatic (mean field) potential, and third, the difference between the exact kinetic energy of interacting system and the Kohn-Sham noninteracting kinetic energy $T_s\left[n\left(\mathbf{r}\right)\right]$.

The most important approximations for $E_{xc}\left[n\left(\mathbf{r}\right)\right]$ suggested by Kohn and Sham [27], is known as the local density approximation, or LDA:

$$E_{xc}\left[n\left(\mathbf{r}\right)\right]\simeq\int\epsilon_{xc}\left(n\left(\mathbf{r}\right)\right)n\left(\mathbf{r}\right)d^3r, \tag{2.69}$$

where $\epsilon_{xc}\left(n\left(\mathbf{r}\right)\right)$ is the exchange-correlation energy per electron in a uniform electron gas. The non-uniform electron gas at $\mathbf{r}$ is therefore treated as if it were

part of a uniform electron gas of constant density $n = n(\mathbf{r})$. This quantity is known exactly in the limit of high density, and can be computed accurately at densities of interest, using Monte Carlo techniques. It is clear that LDA is accurate when the electron density is almost uniform, but it also gives very good results for many atomic, and molecular systems. In practice, one usually employs parametric formulas for $\epsilon_{xc}(n(\mathbf{r}))$.

The extension of LDA to spin-polarized systems, known as the local spin-density approximation (LSDA), has also proven very successful. In fact, the spin-dependent exchange-correlation energy $E_{xc}[n_\uparrow, n_\downarrow]$ can be a better description of the real system than the ordinary $E_{xc}[n(\mathbf{r})]$. The spin dependence allows Hund's rule to be discussed within DFT.

Chapter 3

Quantum Dots

In this chapter, we will first present some selected experiments which have been done so far on quantum-dot systems. Then, we will discuss how the ground-state electronic structures of quantum dots can be described within the single-electron model.

3.1 Experiments

With the development of microfabrication technology, there have been many methods which can be used to produce quantum-dot structures. One of the most direct and flexible way is to laterally pattern existing quantum well structures by etching techniques.

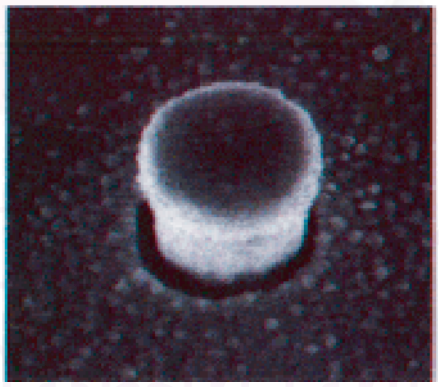

Figure 3.1: A circular quantum dot of the etched type

This section is intended to provide an overview of achieved experimental results showing the quantum-dot ground states under the influence of an external

magnetic field. Many experiments, which have been done over the past decade, used single-electron tunnelling spectroscopy to probe the electronic structures of quantum dots. The achieved results revealed an existence of discrete energy levels in quantum dot structures. However, a clear shell structure of the ground states was first reported by Tarucha *et al* (1996) [1]. In their experiments, the ground-state energy was measured by using the device as shown in Figure 3.2.

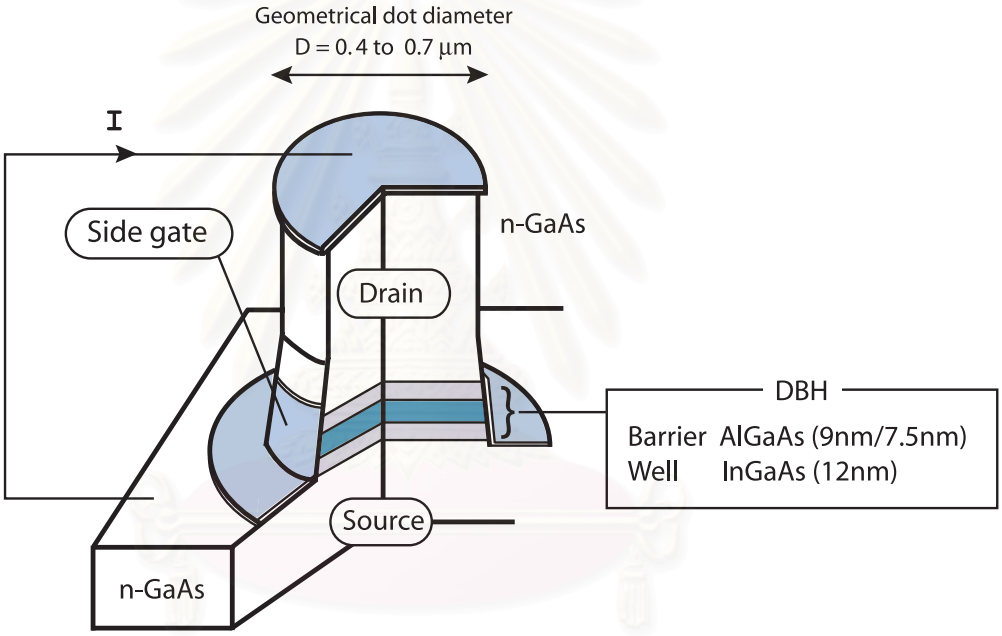

Figure 3.2: The schematic illustration of the experimental setup. The double-barrier heterostructure (DBH) consists of an undoped 12.0 nm. $In_{0.05}Ga_{0.95}As$ well and undoped $Al_{0.22}Ga_{0.78}As$ barriers of thickness 9.0 and 7.5 nm. The source and drain contacts are made from *n*-GaAs [1].

The device was used to study the energy levels and properties of the electrons which are confined vertically between two AlGaAs barriers and laterally in the region of the pillar. The sample was cooled down to 50 mK, and the

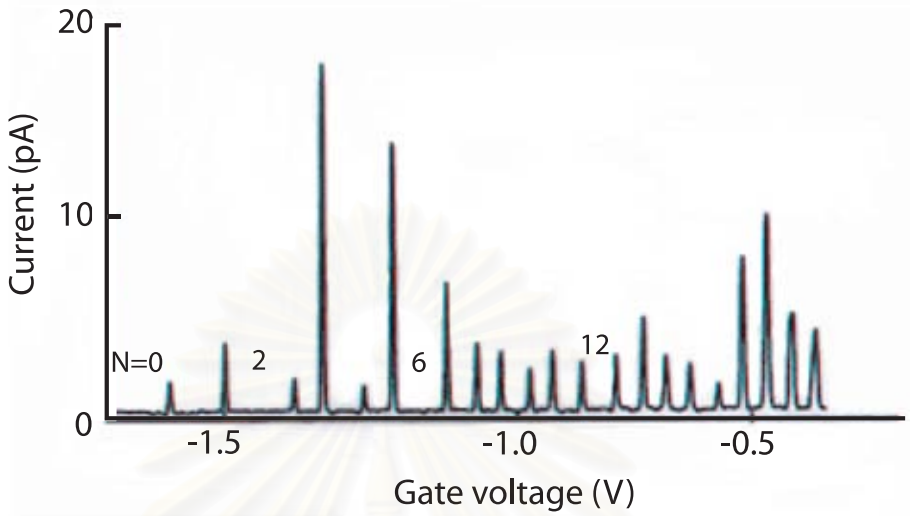

Figure 3.3: Experimental data of current vs gate voltage for a quantum dot with diameter $D = 0.5\ \mu m$ measured by Tarucha *et al* [1].

tunnelling current I flowing through the dot was measured as a function of the gate voltage V_g in response to a small dc voltage applied between the contacts.

In their paper, they pointed out that each peak in the I-V characteristics corresponds to a change of exactly one electron in the dot and the clear Coulomb oscillations are observed for $V_g > -1.6$ V. In other words, the number of electrons N in the dot was varied one by one while the gate voltage was changed. For example, $N = 1$ between the first and second peaks, $N = 2$ between the second and third peaks, etc. We can see that the space between each peak is not constant, the gap is wider when $N = 2$, 6, and 12. The spacing between the current peaks gives the measure of the addition energy (see Figure 3.4). For example, the energy to add the third electron to a 2-electron quantum dot can be derived from the spacing between the second and third peaks.

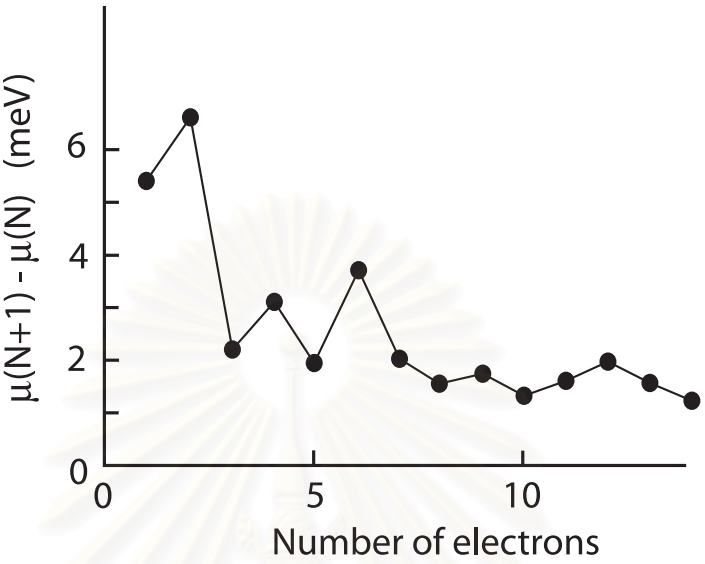

Figure 3.4: Addition energy measured by Tarucha *et al*[1].

As a conclusion, Tarucha *et al* have investigated the ground-state of N-electron quantum dot weakly coupled to the contacts by monitoring the current flowing vertically through the dot at or below 0.3 K as the gate voltage was varied. They pointed out that N can be increased one-by-one starting from zero by making the gate voltage more positive.

3.2 Theoretical Explanation

In order to study the energy levels or other properties of the electrons confined in quantum dots, most theoretical calculations use the effective-mass approximation to simplify the problem. Within this approximation, the electron mass m_e is replaced by the effective mass m_e^* and the effect of the ion cores in crystal structure is taken into account via m_e^* (See Appendix A). The remaining part which have

not been included, is the background confining potential and other external field.

What is the confining potential seen by electrons in the quantum dot? To answer this question, it may be helpful to analyze the quantum-dot structure in details again. As noted briefly in the previous section, quantum dots are made of semiconductor layers, the electrons of interest are confined in the InGaAs well. We know that electrons in semiconductor have energies that are limited to allowed bands separated from each other by band gaps. The highest energy bands containing electrons are of greatest interest. At 0 K the electron density is such that the highest band containing electrons is completely filled up. The next band is completely empty, and the two bands are separated by a band gap. The highest occupied band is called the valence band, while the upper unfilled band is called the conduction band. Electrons in the valence band can be excited to the conduction band by gaining energy from the environment. Both the electrons in the conduction band and the vacant orbitals (holes) left behind in the valence band contribute to the electrical conductivity.

In the vertical quantum dot studied by Tarucha *et. al.*, the heterostructure was created in such a way that a double barrier is formed in the conduction bands (see Figure 3.5). The electrons in the conduction band are therefore confined in the well region. In other words, they are unable to move freely in the crystal growth (vertical) direction.

To model quantum dots of this type, we assume that the confining potential can be separated into a vertical (z) component and a lateral ($\mathbf{r} = (\mathbf{x}, \mathbf{y}) = (\mathbf{r}, \phi)$) component. The confining potential in the vertical direction can be thought of as being a narrowed infinite square well so that the energy level of the first excited state in the z direction is much greater than many of the low energy states in

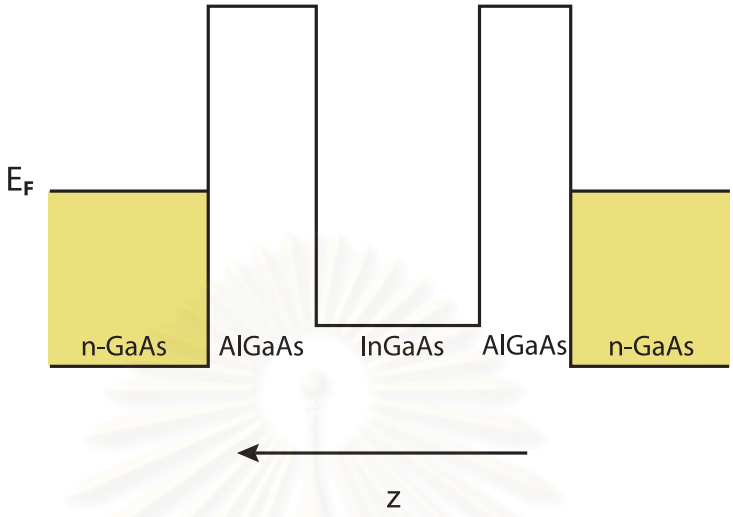

Figure 3.5: Schematic of the double-barriers formed in the conduction band.

the x-y plane. This allows us to model electron motion in a quantum dot as two-dimensional.

Until now, quantum dots of various geometries have been created and studied, for example, rectangular, triangular and circular dots. However, we will focus, for now, on circular quantum dots. Most of theoretical calculations often assume the lateral confining potential $V(r)$ to be parabolic in order to study the electronic structure of a circular dot.

3.2.1 Single-Electron Models

Of course, there are many electrons in the quantum dot system. But, if we ignore, for the moment, the interaction between electrons in the dot, we can gain a lot of information from the analytic solutions of the single-electron Schrodinger equation. The case of a single electron in an isotropic 2D harmonic confining potential under a B field was dealt with many years ago by Fock (1928) [9] and

Darwin (1930) [10]. If the confining potential is written in the form $V(r) = \frac{1}{2}m\omega_0^2 r^2$, the energy levels of the electron is given by

$$E_{n,m} = (2n + |m| + 1)\hbar(\frac{1}{4}\omega_c^2 + \omega_0^2)^2 - \frac{1}{2}l\omega_c, \tag{3.1}$$

where ω_c is the Cyclotron frequency, n the radial quantum number $(= 0, 1, 2, ...)$, and $m = 0, \pm1, \pm2, ...$ Spin is neglected so each states is twofold degenerate. In the absence of the B field, the energy of electron can be simply written as

$$E_{n,m} = (2n + |m| + 1)\hbar\omega_0. \tag{3.2}$$

Therefore, the first state has energy $E_{0,0} = \hbar\omega_0$, the second and third states have energy $E_{0,1} = E_{0,-1} = 2\hbar\omega_0$, and so on. This leads to a complete filling of shells for 2, 6, 12, ... electrons. The experiments of Tarucha *et al* [1] also shows a maximum in the addition energies when the electron number coincides with N = 2, 6, 12, ...

3.2.2 Single Electron Tunnelling

One may ask now what is the correspondence between the peaks occur in the I-Vg characteristic and the energy levels of the electrons confined in the quantum dot region. To answer this question, it is useful to recall the knowledge of tunnelling phenomena particularly in the case of double barriers.

Normally the tunnelling problems involve the propagation of a particle with energy E through a region of potential V, where $E < V$. The particle of interest may initially occupy a free state on the first region, and the tunnelling problem involves the particle coming from this region from the left of a potential barrier and tunnelling through the barrier with a finite probability.

In the well region between two potential barriers, one has quasi-bound states with energies $E1$, $E2$, ... (see Figure 3.6 [31].). If the barriers were infinitely thick, these states would simply be the bound states in a quantum well. However, because of the finite barrier thickness, an electron can still transmit into or out of the well region. But, The transmission can occur only when the energy of the electron (approaching from the region A) approaches one of the quasi-bound energies.

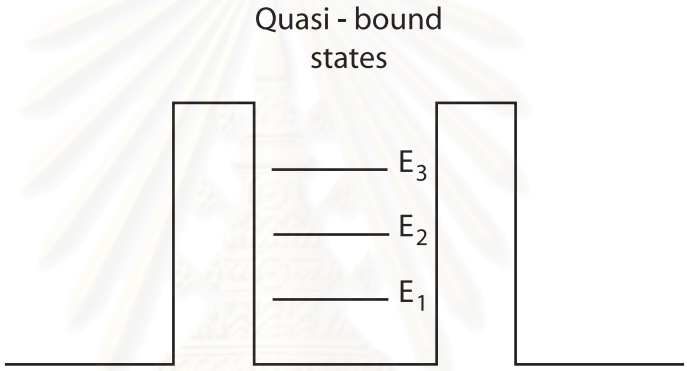

Figure 3.6: Schematic of a double-barrier potential. In the well formed between the two barriers, one has quasi-bound states with energies E1, E2, ... As the energy of an electron in region A approaches these energies, the tunnelling probability approaches unity

Similarly, an electron can tunnel into a quantum dot only if the Fermi energy of an electron in the contact region lines up with an energy level of the quantum-dot system. In practice, the energy levels were shifted by tuning the external electrostatic potential from the side gate. For example, by increasing the gate voltage, the levels of the quantum dot are shifted in energy relative to the Fermi level of the contact region. This allows the number of electrons confined in the quantum dot to increase one by one. Tunnelling through excited states of

a quantum dot was observed for various tunnelling barriers many years ago by Weis et al (1993) [32].

Chapter 4

N-Electron Models: Density Functional Approach

The single-electron model which was reviewed in chapter 3 can give us only a simple qualitative explanation of real quantum dots. To describe the electronic structure of quantum-dot systems, one must go beyond the non-interacting electron model.

In this chapter, we will briefly describe how the density functional theory presented in chapter 2 can give us a better explanation of the ground-state electronic structures of N-electron quantum dots. The methodology based on the spin-polarized Kohn-Sham scheme will be presented and used as a basis for numerical calculations.

4.1 Methodology

To obtain the ground-state energies and densities of the N-electron quantum dot, we solve the self-consistent spin-polarized Kohn-Sham equations (Eq. 2.64)

$$\left[-\frac{1}{2}\nabla^2 + v_{eff}^{(\sigma)}(\mathbf{r})\right]\varphi_i^{(\sigma)}(\mathbf{r}) = \varepsilon_i^{(\sigma)}\varphi_i^{(\sigma)}(\mathbf{r}), \tag{4.1}$$

where $\mathbf{r} = (x, y)$ and the index σ accounts for the spin ($\uparrow$ or $\downarrow$). Here, the rescaled atomic units are used, with lengths in units of the effective Bohr radius $a_0^* = 4\pi\epsilon\hbar^2/m_e^* e^2$ and energy in effective atomic units of energy called Hartree* (see Appendix B).

The spin-dependent effective potentials $v_{eff}^{(\sigma)}(\mathbf{r})$ contains contributions from the external confining potential $v(\mathbf{r})$, the classical electrostatic (Hartree) potential of the electrons, and the exchange-correlation potential $v_{xc}^{(\sigma)}$.

$$v_{eff}^{\sigma}(\mathbf{r}) = v(\mathbf{r}) + \int \frac{n(\mathbf{r}')}{|\mathbf{r}-\mathbf{r}'|} d^2r' + v_{xc}^{\sigma}(\mathbf{r}; [n_\uparrow, n_\downarrow]), \tag{4.2}$$

where

$$n_\sigma(\mathbf{r}) = \sum_{i=1}^{N_\sigma} \left|\varphi_i^{(\sigma)}(\mathbf{r})\right|^2, \quad n(\mathbf{r}) = n_\uparrow(\mathbf{r}) + n_\downarrow(\mathbf{r}). \tag{4.3}$$

4.1.1 Local-Spin Density Functional Approximation

The approximate exchange-correlation energy functional used in this thesis is the so-called local-spin-density approximation (LSDA).

$$E_{xc}^{LSDA}[n_\uparrow, n_\downarrow] = \int \epsilon_{xc}([n_\uparrow, n_\downarrow]; \mathbf{r})\, n(\mathbf{r})\, d^2r, \tag{4.4}$$

where $\epsilon_{xc}([n_\uparrow, n_\downarrow]; \mathbf{r})$ is the exchange-correlation energy per particle of a uniform electron gas of density n. This quantities can be computed accurately at densities of interest using Monte Carlo techniques. Note that the exchange-correlation potential defined in Eq. (2.67) is now given by

$$v_{xc}^{\sigma}(\mathbf{r}; [n_\uparrow, n_\downarrow]) = \frac{\partial [n\epsilon_{xc}]}{\partial n_\sigma} \tag{4.5}$$

and the corresponding expression for the ground-state energy is:

$$\begin{aligned} E[n_\uparrow, n_\downarrow] &= \sum_{i=1}^{\infty}\sum_{\sigma} \varepsilon_i^{(\sigma)} - \frac{1}{2}\int \frac{n(\mathbf{r})\, n(\mathbf{r}')}{|\mathbf{r}-\mathbf{r}'|} d^2r d^2r' - \sum_{\sigma}\int v_{xc}^{(\sigma)}([n_\uparrow, n_\downarrow]; \mathbf{r})\, n_\sigma(\mathbf{r})\, d^2r \\ &\quad + \int \epsilon_{xc}([n_\uparrow, n_\downarrow]; \mathbf{r})\, n(\mathbf{r})\, d^2r, \end{aligned} \tag{4.6}$$

where the second term subtracts half of the double counting of the electrostatic energy, and the last term is a similar substraction for the exchange-correlation energy. The numbers of electrons with ↑ spin and ↓ spin need to be varied to achieve minimum total energy.

4.1.2 Analytic Parametization for ϵ_{xc}

In this thesis, we employ the new parametrized form of ϵ_{xc} recently proposed by Attaccalite *et al* (2002) [12]. Note that this new parametrization is an extension to the most used parametrized form of Tanatar and Ceperly [11] which based on diffusion Quantum Monte Carlo (DMC) data at spin polarization $\zeta = 0$ and $\zeta = 1$.[3]

Attaccalite *et al* [12] have presented new diffusion Quantum Monte Carlo simulations for a wide range of electron densities r_s and spin polarizations ζ. This direct DMC calculation of ζ dependence is new and provides a reliable basis for building an LSD energy functional for 2D systems. The new parametrization of ϵ_{xc} is written as

$$\begin{aligned}\epsilon_{xc}(r_s,\zeta) &= \epsilon_x(r_s,\zeta)+\epsilon_c(r_s,\zeta)\\ &= \epsilon_x(r_s,\zeta)+\left(e^{-\beta r_s}-1\right)\epsilon_x^{(6)}(r_s,\zeta)+\alpha_0(r_s)+\alpha_1(r_s)\zeta^2+\alpha_0(r_s)\zeta^4,\end{aligned} \tag{4.7}$$

where r_s is the density parameter and

$$\epsilon_x^{(6)}(r_s,\zeta)=\epsilon_x(r_s,\zeta)-\left(1+\frac{3}{8}\zeta^2+\frac{3}{128}\zeta^4\right)\epsilon_x(r_s,0) \tag{4.8}$$

[3]The two-dimensional (2D) electron gas at T=0 is characterized only by two parameters: the spin polarization $\zeta = (n_\uparrow - n_\downarrow)/n$ and the density parameter $r_s = 1/\sqrt{\pi n}$ (The radius of the circle that encloses one particle on the average).

is the Taylor expansion of ϵ_x beyond fourth order in ζ. The exchange term is given by

$$\epsilon_x(r_s,\zeta) = -\frac{2\sqrt{2}}{3\pi r_s}\left((1+\zeta)^{3/2}+(1-\zeta)^{3/2}\right). \tag{4.9}$$

The density dependent function $\alpha_i(r_s)$ is a generalization of the Perdew-Wang [33] form to the 2D case,

$$\alpha_i(r_s) = A_i + \left(B_i r_s + C_i r_s^2 + D_i r_s^3\right)\ln\left(1+\frac{1}{E_i r_s + F_i r_s^{3/2} + G_i r_s^2 + H_i r_s^3}\right). \tag{4.10}$$

The optimal values of the parameters are listed in Table 4.1. This new functional includes several known high- and low-density limits.

	i=0	i=1	i=2
A_i	-0.1925	0.117331	0.0234188
B_i	0.0863136	-3.394×10^{-2}	-0.03709.
C_i	0.057234	-7.66765×10^{-3}	0.0163618
E_i	1.0022	0.4133	1.424301
F_i	-0.02069	0	0
G_i	0.340	6.68467×10^{-2}	0
H_i	1.747×10^{-2}	7.799×10^{-4}	1.163099

Table 4.1: Optimal fit parameters for the correlation energy as parametrized in Eq. (4.7) and (4.10). The parameter $D_i = -A_i H_i$, and β is equal to 1.3386.

4.1.3 LSD Correlation Potential

The LSD correlation potential v_c^σ for electrons of spin σ is given by

$$v_c^\sigma(r_s,\zeta) = \frac{\partial[n\epsilon_c]}{\partial n_\sigma} = \epsilon_c(r_s,\zeta) - \frac{r_s}{2}\frac{\partial\epsilon_c(r_s,\zeta)}{\partial r_s} - (\zeta - \mathrm{sgn}\ \sigma)\frac{\partial\epsilon_c(r_s,\zeta)}{\partial\zeta}. \tag{4.11}$$

where sgn σ is +1 for spin-up electrons and -1 for spin-down electrons. From the analytic representations of ϵ_{xc} in Eq. (4.7)-(4.9), one can rewrite the expression for $\epsilon_c(r_s,\zeta)$ as follows

$$\epsilon_c(r_s,\zeta) = \frac{2\sqrt{2}}{3\pi r_s} F(\zeta)\left(1-e^{-\beta r_s}\right) + \alpha_0(r_s) + \alpha_1(r_s)\zeta^2 + \alpha_2(r_s)\zeta^4, \tag{4.12}$$

where

$$F(\zeta) = (1+\zeta)^{3/2} + (1-\zeta)^{3/2} - \left(2 + \frac{3}{4}\zeta^2 + \frac{3}{64}\zeta^4\right). \tag{4.13}$$

Therefore, the derivative with respect to r_s is

$$\frac{\partial\epsilon_c(r_s,\zeta)}{\partial r_s} = \frac{2\sqrt{2}}{3\pi} F(\zeta)\frac{\left[e^{-\beta r_s}(1+\beta r_s)-1\right]}{r_s^2} + \alpha_0'(r_s) + \alpha_1'(r_s)\zeta^2 + \alpha_2'(r_s)\zeta^4, \tag{4.14}$$

where

$$\begin{aligned} \alpha_i'(r_s) &= \frac{d\alpha_i(r_s)}{dr_s} \qquad (4.15)\\ &= \left(B_i + 2C_i r_s + 3D_i r_s^2\right)\ln\left(1+\frac{1}{f_i(r_s)}\right) - \frac{\left(B_i r_s + C_i r_s^2 + D_i r_s^3\right) f_i'(r_s)}{f_i(r_s)\left(f_i(r_s)+1\right)} \end{aligned}$$

$$f_i(r_s) = E_i r_s + F_i r_s^{3/2} + G_i r_s^2 + H_i r_s^3 \tag{4.16}$$

$$f_i'(r_s) = E_i + \frac{3}{2}F_i r_s^{1/2} + 2G_i r_s + 3H_i r_s^2. \tag{4.17}$$

The derivative w.r.t. ζ is simply

$$\frac{\partial\epsilon_c(r_s,\zeta)}{\partial\zeta} = \frac{2\sqrt{2}}{3\pi r_s}\left(1-e^{-\beta r_s}\right)F'(\zeta) + 2\alpha_1(r_s)\zeta + 4\alpha_2(r_s)\zeta^3 \tag{4.18}$$

$$F'(\zeta) = \frac{3}{2}\left((1+\zeta)^{1/2} + (1-\zeta)^{1/2}\right) - \frac{3}{2}\zeta - \frac{3}{16}\zeta^3. \tag{4.19}$$

4.2 Procedure

In order to minimize the energy functional $E[n_\uparrow, n_\downarrow]$, the spin-polarized Kohn-Sham equations have to be solved self-consistently. The general procedure is decribed as followed:

1. Define mesh on 2D region, boundary conditions, and the coefficients.

2. Start from an initial guess of the effective potential which was chosen to be the confining potentials.

3. Compute the spin-polarized Kohn-Sham equations.

$$\left[-\frac{1}{2}\nabla^2 + v_{eff}^{(\sigma)}(\mathbf{r})\right]\varphi_i^{(\sigma)}(\mathbf{r}) = \varepsilon_i^{(\sigma)}\varphi_i^{(\sigma)}(\mathbf{r})$$

4. Calculate new density

$$n_\sigma(\mathbf{r}) = \sum_{i=1}^{N_\sigma}\left|\varphi_i^{(\sigma)}(\mathbf{r})\right|^2, \quad n(\mathbf{r}) = n_\uparrow(\mathbf{r}) + n_\downarrow(\mathbf{r})$$

and effective potential,

$$v_{eff}^{\sigma}(\mathbf{r}) = v(\mathbf{r}) + \int \frac{n(\mathbf{r}')}{|\mathbf{r}-\mathbf{r}'|}d^2r' + v_{xc}^{\sigma}(\mathbf{r};[n_\uparrow, n_\downarrow]).$$

5. Calculate total energy

$$\begin{aligned} E[n_\uparrow, n_\downarrow] &= \sum_{i=1}^{\infty}\sum_{\sigma}\varepsilon_i^{(\sigma)} - \frac{1}{2}\int\frac{n(\mathbf{r})\,n(\mathbf{r}')}{|\mathbf{r}-\mathbf{r}'|}d^2r\,d^2r' - \sum_{\sigma}\int v_{xc}^{(\sigma)}([n_\uparrow, n_\downarrow];\mathbf{r})\,n_\sigma(\mathbf{r})\,d^2r \\ &\quad + \int \epsilon_{xc}([n_\uparrow, n_\downarrow];\mathbf{r})\,n(\mathbf{r})\,d^2r, \end{aligned}$$

If energy changed substantially, go to step 3.

6. If energy converged calculate addition energy and other properties

In the calculation we used a mixing scheme where the new effective potential V^{i+1} is obtained from the input and output potentials according to

$$V_{in}^{i+1} = (1-a)V_{in}^{i} + aV_{out}^{i}. \tag{4.20}$$

Implementation of this procedure was performed with Matlab version 5.3.1 pde-toolbox[4] which is based on finite-element method (FEM).

[4]A user-friendly interface based on Matlab v.4.2 pde-toolbox for simulating time-dependent problems and time-independent eigenvalue problems of single electron in two dimensions can be found in Ref [34].

Chapter 5

Results and Discussion

5.1 Harmonic Confinement

We first present calculated results for 2D harmonic potential $V_p = \frac{1}{2}k^2r^2$. The attraction of this model is that an analytic solution to the single electron Schrodinger equation exists. So, the single electron solution can serve as a basis for studying of N-electron systems. In addition, it can be a good test case to gauge the accuracy of different approaches.

5.1.1 Addition Energy Spectrum

The addition energy is the change of chemical potential:

$$\Delta\mu(N) = \mu(N+1) - \mu(N) \tag{5.1}$$

where $\mu(N)$ is the chemical potential. The chemical potential which is defined as $\mu(N) \equiv E(N) - E(N-1)$ is the energy required to add one electron to the system with $N-1$ electrons.

Experimentally, Tarucha *et al* [1] found that the addition energy was unusually large for N = 2, 6, and 12 for the circular quantum dot with D = 0.44 and 0.5 μm. They also observed a relatively large addition energy for N=4 in most devices.

In our calculation, we obtain the expected peaks at N = 2, 6, and 12 (Figure 5.1). In addition, at N = 4, and 9 the smaller peaks can also be noticed.

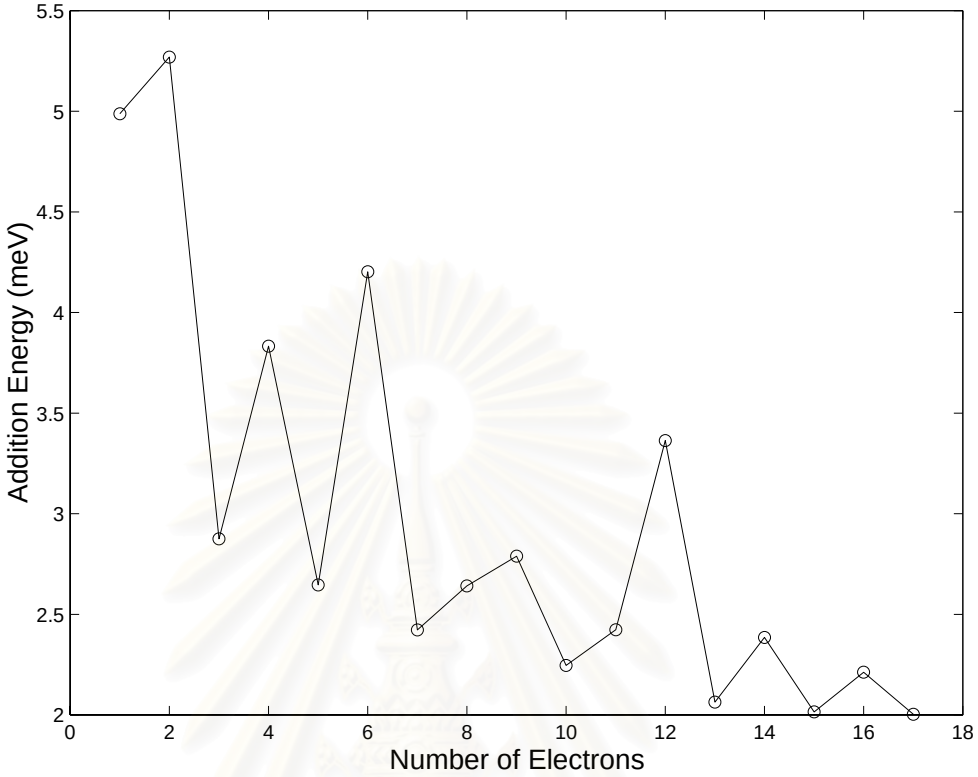

Figure 5.1: The calculated addition energy $(\mu(N+1)-\mu(N))$ of a circular quantum dot with the confining potential specified by $k = 0.3$ (effective atomic unit) or $\hbar\omega = 3.19$ meV.

By comparison with the experimental results of Tarucha *et al* (1996) (Figure 3.4), the energy range of the real quantum dot is lower when the number of electrons is higher, but there is no such effect in Figure 5.1. To understand this, we present here the calculated results for the quantum dots of different widths and depths ($k = 0.3$, 0.6, and 0.9). We can see from Figure 5.2 that the range of the addition energies are shifted down when the values of confinement parameter k are decreased. The cause of this effect is the change in the diameter of the quantum dot while a negative voltage is applied to the side gate. In other words, the diameter of the dot becomes smaller which corresponds to the increasing in the value of k.

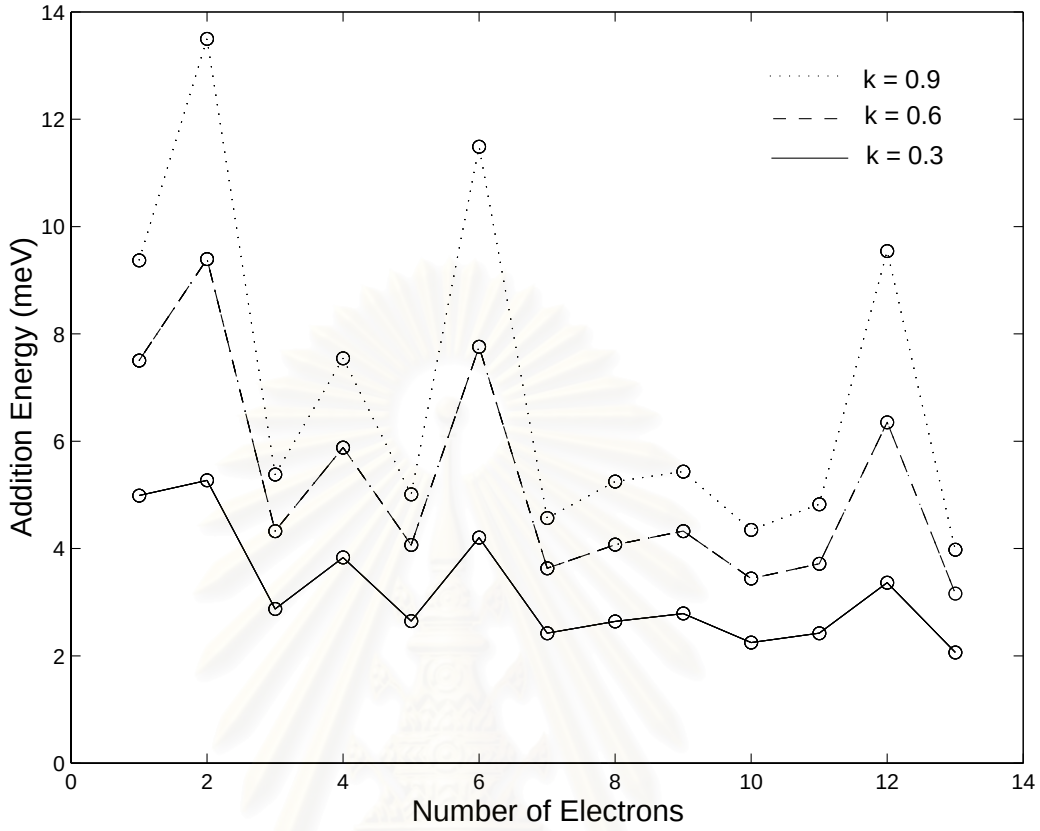

Figure 5.2: The effect of the confinement parameter k on the addition energy spectra.

If we ignore the interaction of electrons for the moment, it is clear that the energy differences between each single-particle states become smaller when the depth of a quantum dot is decreased (Eq. 3.2). We decrease the confinement parameter (k) further to see the effect of the energy-level spacing. The calculated results of the addition energy spectra are shown in Figure 5.3. One can see that the peak at $N = 2$ begins to disappears at $k = 0.2$. This shows the effect of the electron interaction which becomes more important when the energy-level spacing is small compared to the total energy.

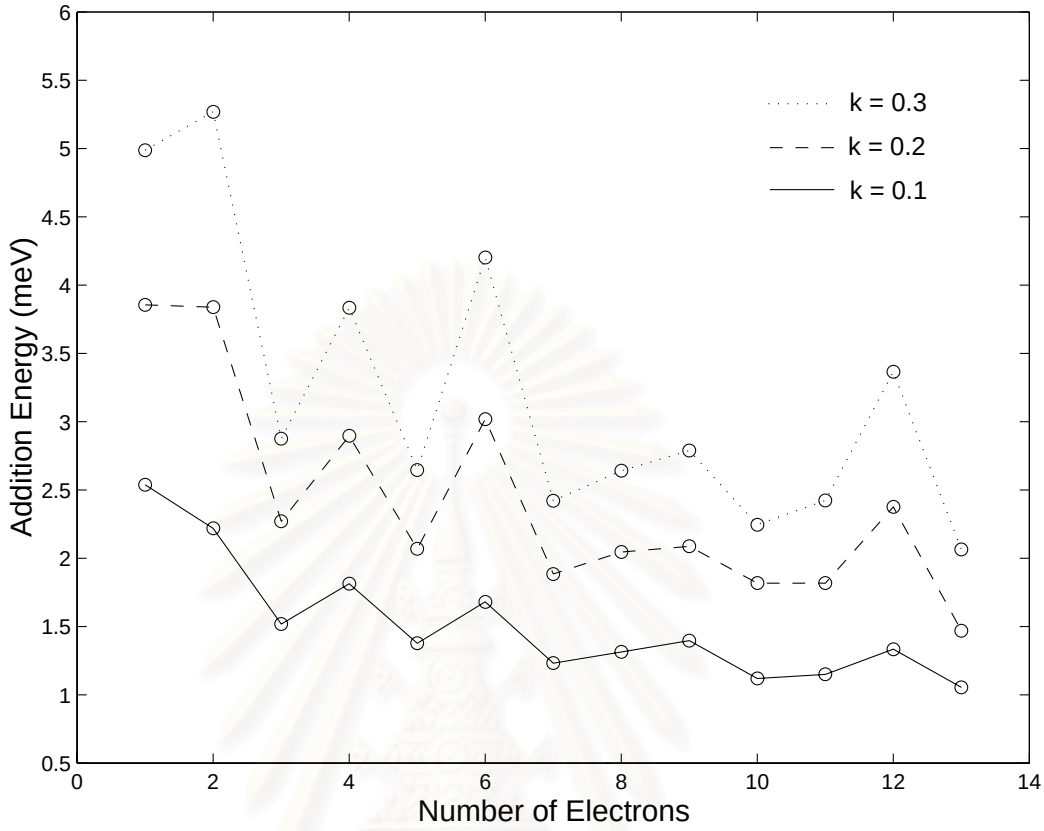

Figure 5.3: The addition energy $(\mu(N+1) - \mu(N))$ of a quantum dot with the confining potential specified by $k = 0.3$, 0.2, and 0.1.

5.1.2 Electron Density

As shown in Figure 5.1-5.2, the addition energy will be unusually large at N=2, 6, and 12. We find that this corresponds to the zero total spin electronic states $(N_\uparrow = N_\downarrow)$. The electron densities of these states are shown in Fig 5.4. We can see that the electrons in a circularly shaped confinement form rotationally symmetric distribution. At N=2, the electron densities have the maximum value at the center of the confinement. While at N=6, the electron densities are small in the center of the dot due to the increasing of the electron-electron interaction.

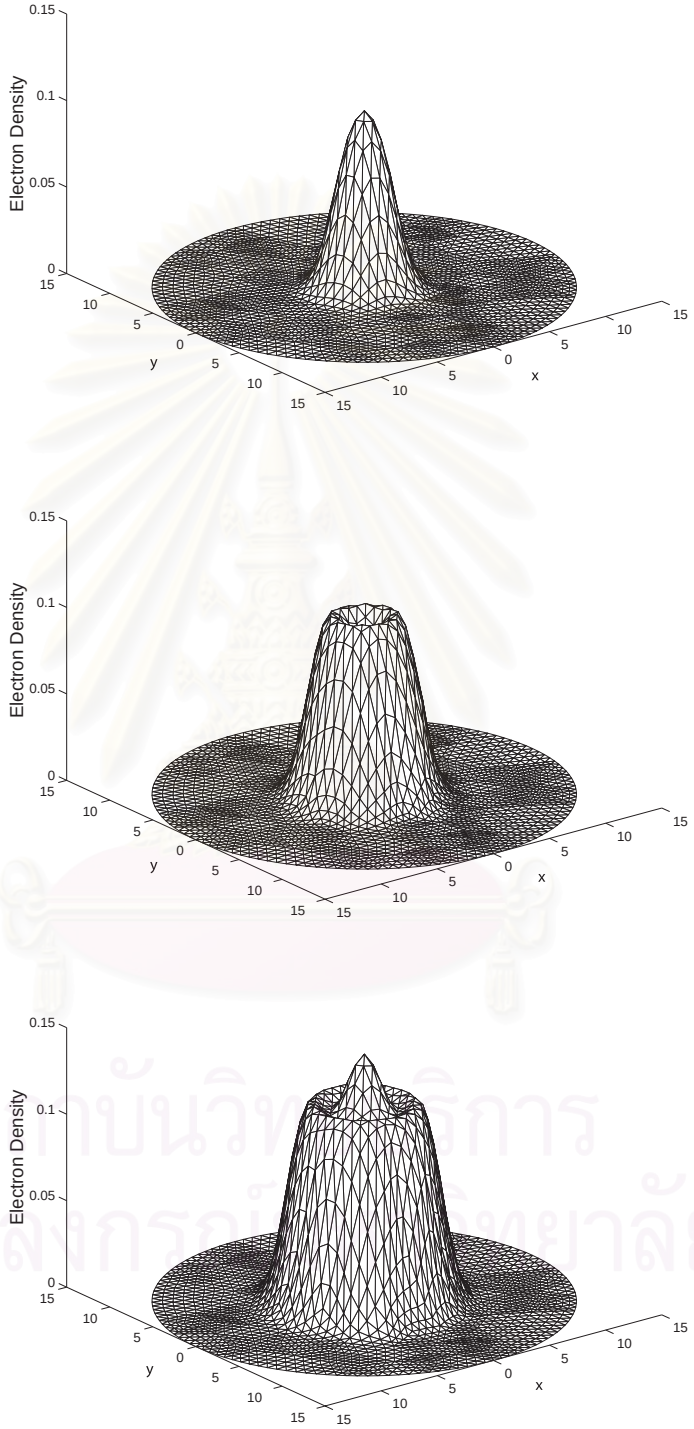

Figure 5.4: The electron densities at N = 2, 6, and 12 through the center of a harmonic quantum dot with $k = 0.3$.

5.1.3 Spin Polarization

To see how an electron fills in a quantum dot, we plot the spin polarization $((N_\uparrow - N_\downarrow)/(N_\uparrow + N_\downarrow))$ as a function of N (see Figure 5.5). The zero polarization at $N = 2$, 6, 12 corresponds to the full-shells, while the local maximum values at $N = 1$, 4, 9 corresponds to half-filled shells.

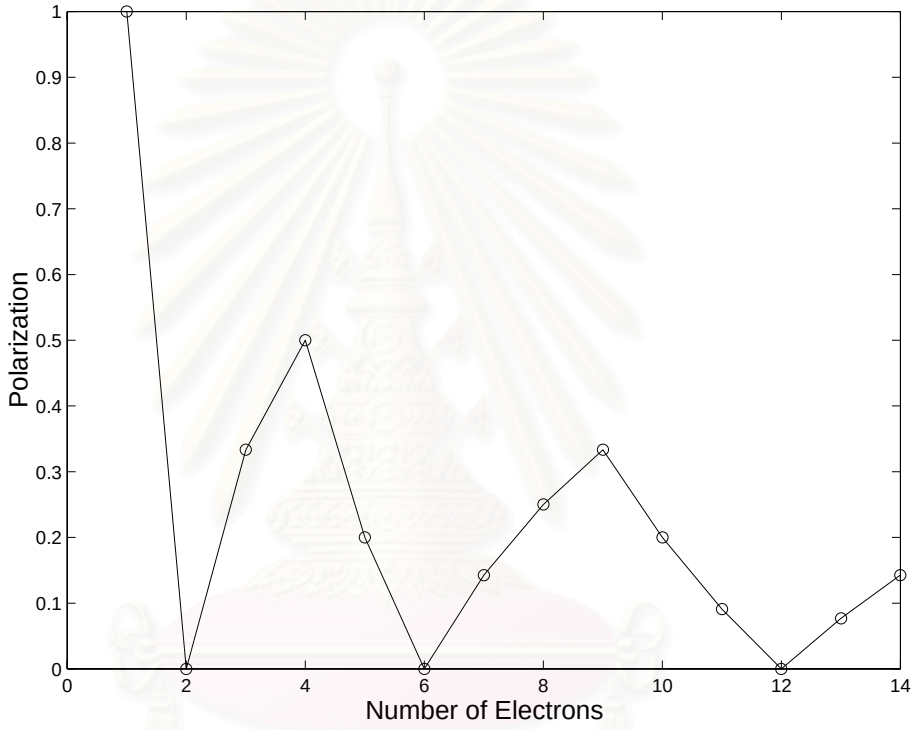

Figure 5.5: The spin polarization of the electronic states defined as a ratio $(N_\uparrow - N_\downarrow)/(N_\uparrow + N_\downarrow)$ of electrons with spins up $(N_\uparrow)$ and down $(N_\downarrow)$.

By analogy to atoms, we find that Hund's rule also apply in a quantum-dot as well as in an atom. According to Hund's rule, as degenerate states are filled, electrons enter the dot with parallel spins until the degenerate states is half-full resulted in the maximum value of total spin (see Table 5.1). For example, the total energy of the spin configuration $(N_\uparrow, N_\downarrow) =$ (6,3) is lower than that of the spin configuration (5,4) at electron number N=9. That means the electronic state

Energy	$\hbar\omega_0$	$2\hbar\omega_0$		$3\hbar\omega_0$		
N	$E_{0,0}$	$E_{0,1}$	$E_{0,-1}$	$E_{0,2}$	$E_{0,-2}$	$E_{1,0}$
1	$\uparrow$					
2	$\uparrow\downarrow$					
3	$\uparrow\downarrow$	$\uparrow$				
4	$\uparrow\downarrow$	$\uparrow$	$\uparrow$			
5	$\uparrow\downarrow$	$\uparrow\downarrow$	$\uparrow$			
6	$\uparrow\downarrow$	$\uparrow\downarrow$	$\uparrow\downarrow$			
7	$\uparrow\downarrow$	$\uparrow\downarrow$	$\uparrow\downarrow$	$\uparrow$		
8	$\uparrow\downarrow$	$\uparrow\downarrow$	$\uparrow\downarrow$	$\uparrow$	$\uparrow$	
9	$\uparrow\downarrow$	$\uparrow\downarrow$	$\uparrow\downarrow$	$\uparrow$	$\uparrow$	$\uparrow$
10	$\uparrow\downarrow$	$\uparrow\downarrow$	$\uparrow\downarrow$	$\uparrow\downarrow$	$\uparrow$	$\uparrow$
11	$\uparrow\downarrow$	$\uparrow\downarrow$	$\uparrow\downarrow$	$\uparrow\downarrow$	$\uparrow\downarrow$	$\uparrow$
12	$\uparrow\downarrow$	$\uparrow\downarrow$	$\uparrow\downarrow$	$\uparrow\downarrow$	$\uparrow\downarrow$	$\uparrow\downarrow$

Table 5.1: Filling order for electrons in a two-dimensional harmonic confinement. The full-shell filling is corresponding to N=2, 6, 12, ... The electrons will occupy all different degenerate states until the shell is half-full before entering opposite spins.

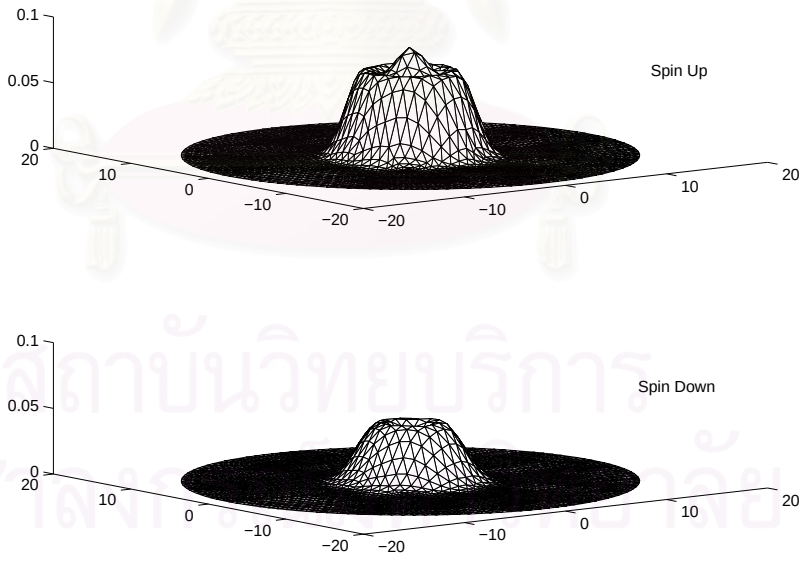

Figure 5.6: The spin-densities of electrons with the spin configuration ($N_\uparrow$, $N_\downarrow$) = (6,3) in the harmonic dot defined by $k = 0.3$.

with spin configuration (6,3) is more stable than the (5,4) state. However, for N=15, we found that the total energy of the spin configuration ($N_\uparrow$, $N_\downarrow$)=(8,7) is slightly lower (0.1 meV) than that of the spin configuration (9,6). The densities of spin-up and spin-down electrons at N=9 are shown in Figure 5.6.

5.2 Energy Contribution

To be able to see quantitatively how much the electron-electron interaction contributes to the total energy, we plot the values of different components of the total energy as a function of N (see Figure 5.7). The leading effect of the interaction is the Hartree energy. By comparison, the correlation energy is obviously smaller than the other components. This can be one of the reason why our calculated results presented in the previous sections are all in a very good agreement with results which have been previously calculated by other groups using the most used form of Tanatar and Ceperley of the exchange-correlation functional [8], [7]. (Note that both forms has the same contribution for the exchange energy, but the correlation part is different: the new representation proposed by Attacalite *et al* [12] was fitted by using the diffusion Quantum Monte Carlo simulations for a wide range of electron densities and spin polarization.)

It is clear that the exchange-correlation effect reduces the total energy values. We find that most of the spin-polarized states ($N_\uparrow \neq N_\downarrow$) has a larger exchange-correlation effect than the spin-compensated states. For example, the calculated exchange-correlation energy E_{xc} of the spin configuration (3,1)is -15.11 meV, while the exchange-correlation energy of the state (2,2) is equal to -15.10 meV.

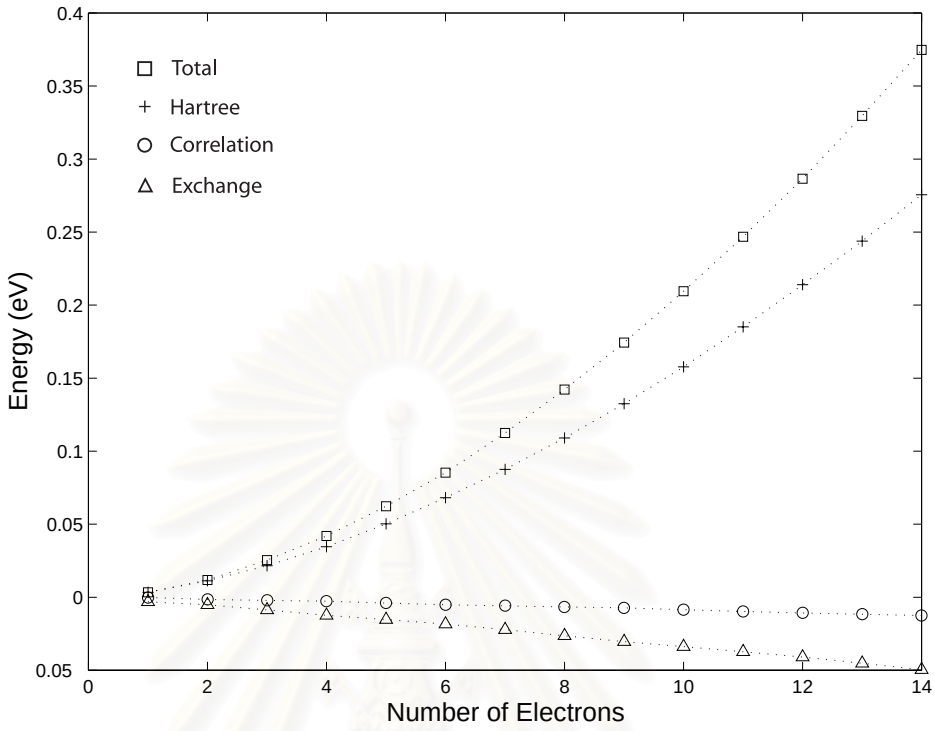

Figure 5.7: Contributions to the ground-state energy of a 2D hamonic dot

5.3 Anisotropic Parabolic Confinement

In this section we present the calculated results of a quantum dot defined by anisotropic parabolic confinement. The main purpose was to examine the effect of geometrically distorting on quantum-dot structures. The 2D anisotropic parabolic confinement is described by the confinement parameters k_x and k_y:

$$V(x,y) = \frac{1}{2}(k_x^2 x^2 + k_y^2 y^2) = \frac{1}{2}k^2(\delta x^2 + \frac{1}{\delta}y^2) \tag{5.2}$$

In order to conserve the area of the quantum dot when the confinement parameters are changed, the ratio of the confinement parameters $\delta = k_x/k_y$ will be used instead.

We now make a comparison between the addition energy spectra of anisotropic

and harmonic confinements. The calculated result for the quantum dot with $\delta = 1.1$ and $k = 0.3$ is shown in Figure 5.8 with circles connected by solid lines. The dotted lines plotted is the addition energy spectra of a harmonic confinement with $k = 0.3$. One can see that the small peak at $N = 9$ is disappeared in this case. This effect may be explained in terms of the single-electron states. When a circular quantum dot is deformed, the cylindrical symmetry will be removed. As a result, we lose some of the degeneracy associated with the isotropic confinement. The calculated spectra shows that the clear shell structure corresponding to $N = 2, 6, 12$ still occurs for the slightly deformed quantum dot with $\delta = 1.1$.

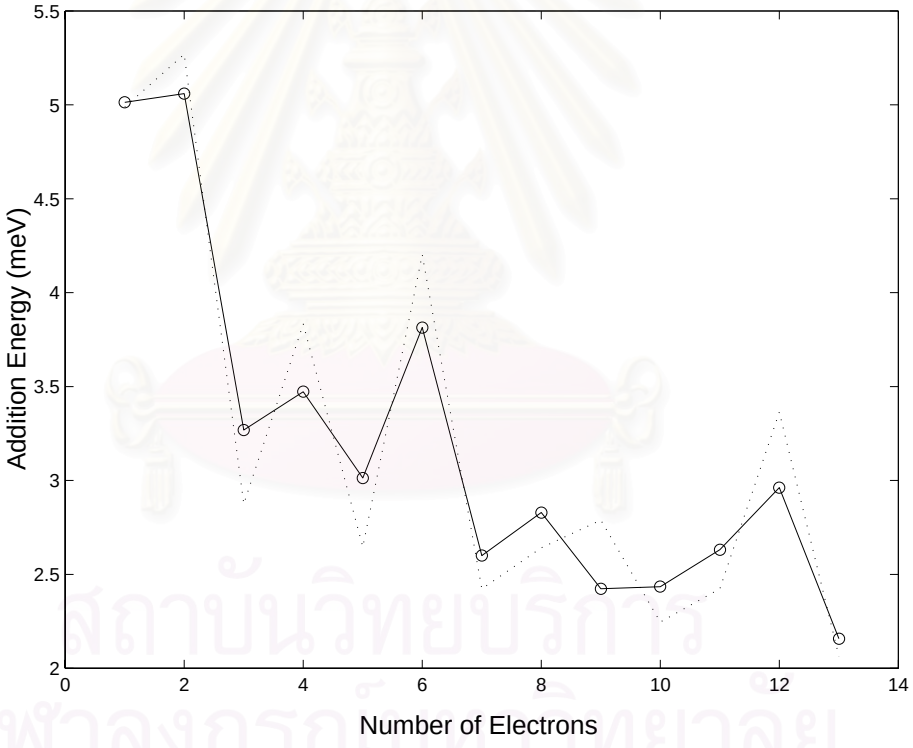

Figure 5.8: The calculated addition energies $(\mu(N+1) - \mu(N))$ of an anisotropic parabolic confinement with $\delta = 1.1$(solid lines) compared with the calculated results of a harmonic confinement (dotted line).

As we increase δ further, the shell structure begins to disappeared. At

$\delta = 1.2$, the peaks in addition energy spectra at $N = 2$, 4, 9, and 12 are no longer to exist (Figure 5.9). One can see small peaks at $N = 6$, and 11 instead.

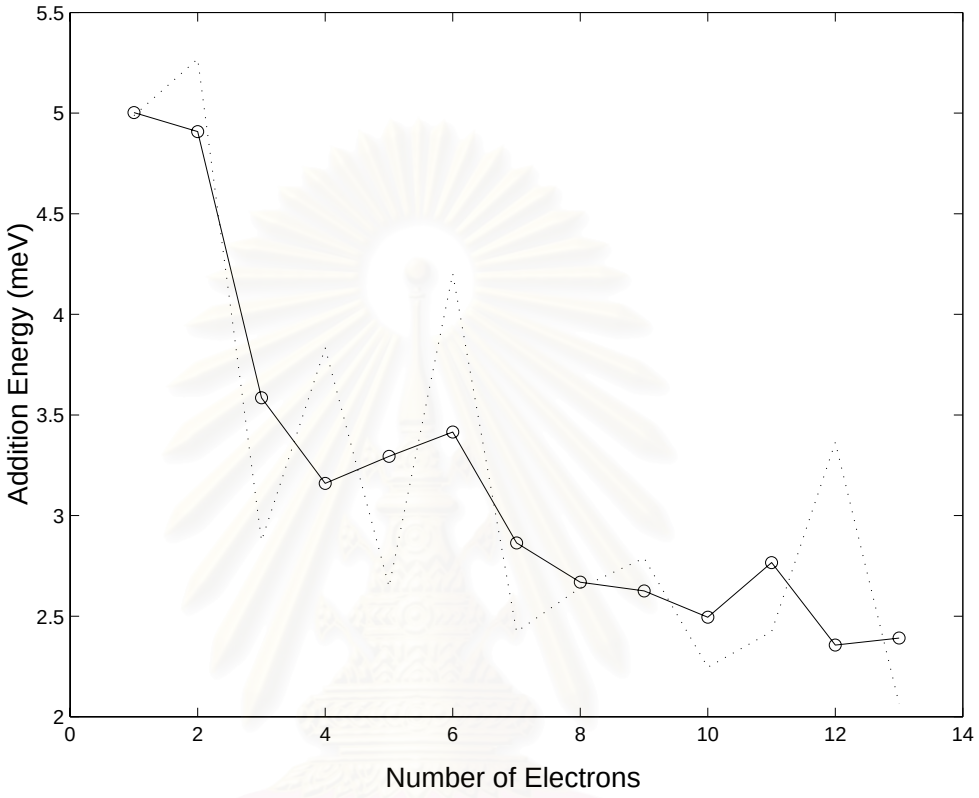

Figure 5.9: The calculated addition energies $(\mu(N+1) - \mu(N))$ of an anisotropic parabolic confinement with $\delta = 1.2$(solid lines) compared with the calculated results of a harmonic confinement (dotted line).

In Sec. 5.1, we have seen that the spin-configuration of electrons in harmonic confinement satisfy Hund's rule. In other words, there is maximum spin polarization for half-filled shells ($N = 4, 9$). Since, some of the degeneracy associated with the circular symmetry may be removed in an anisotropic confinement. The maximum spin polarization at $N = 4, 9$ may not be found. To illustrate, we plot in Figure 5.10 the spin polarization $((N_\uparrow - N_\downarrow)/(N_\uparrow + N_\downarrow))$ as a function of N for the anisotropic confinement with $\delta = 1.1$ and 1.2. The results show that the

slightly distorting ($\delta = 1.1$) of the dot geometry does not change the shell-filling order of electrons in a circular quantum dot. The maximum spin polarization at $N = 9$ begins to disappear when $\delta = 1.2$. Our results agree well with the numerical calculations in Ref. [2].

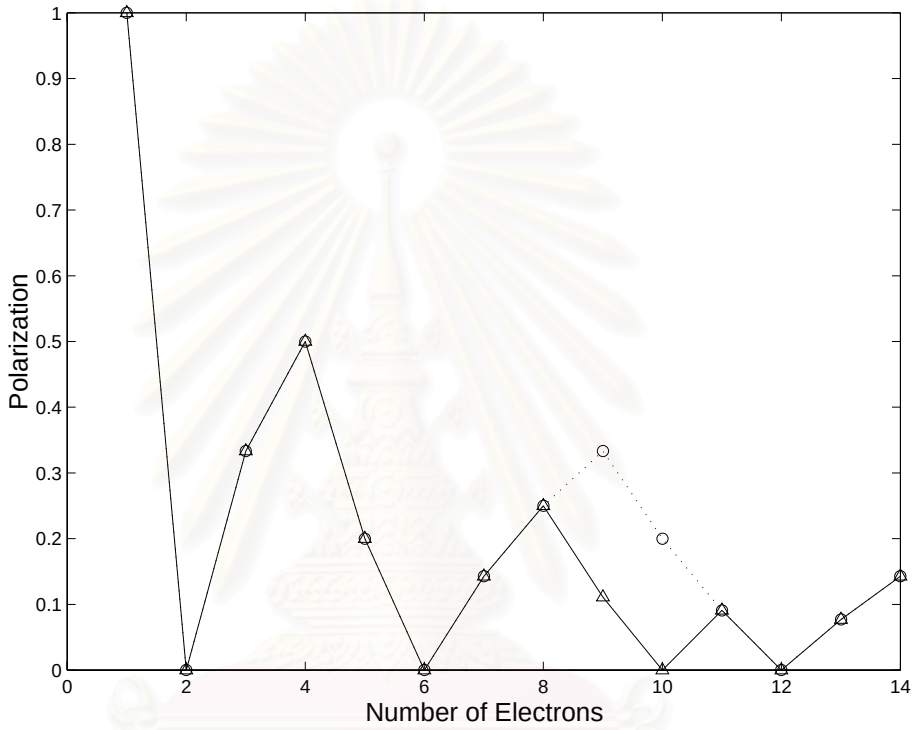

Figure 5.10: The spin polarization $((N_\uparrow - N_\downarrow)/(N_\uparrow + N_\downarrow))$ of anisotropic quantum dots defined by $\delta = 1.1$ (circles) and $\delta = 1.2$ (triangles).

Chapter 6

Conclusions

6.1 Summary

In this thesis, we have studied the electronic structures of a quantum dot by using a numerical method based on the spin-density functional theory. In order to avoid symmetry restriction, the calculations were performed in real space. We developed a computer program based on the finite-element methods using Matlab v5.3. Within the program, the spin-polarized Kohn-Sham equations are solved self-consistently. For the local spin-density approximation of the exchange-correlation energy, we used the recently proposed analytic representation of Attaccalite *et al* instead of the most used form of Tanatar and Ceperley.

To compare with the previously observed experimental results and theoretical calculations, we examined the addition energy spectra (the changes of the chemical potential) of quantum dots defined by harmonic and anisotropic confinements. For Harmonic confinement, the addition energy spectra obtained shows a clear shell structure as a function of N corresponding to the unusually large peaks at N = 2, 6, 12, and the smaller peaks at N = 4, 9. Shell-filling and spin configuration are found to determine mostly by Hund's rule. These findings are in very good agreement with previously observed experimental results. The geometry deformation of the anisotropic parabolic confinement was studied by changing the confinement parameter δ. The comparison between the isotropic

dot with $\delta = 1$ and the anisotropic parabolic dots with $\delta = 1.1$ and 1.2 were performed. The calculated results shows that there still exists the shell structure corresponding to $N = 2$, 6, 12 for the slightly deformed quantum dot with $\delta = 1.1$.

6.2 Future work

Because of the progress in micro-fabrication technology, quantum dots can be created in various shapes and sizes. Further research efforts could attempt to apply this real-space based method to other anisotropic-shaped quantum dots.

References

[1] S. Tarucha, D. G. Austing, T. Honda, R. J. van der Hage, and L. P. Kouwenhoven, *Phys. Rev. Lett.*, 77(17):3613, 1996.

[2] D. G. Austing, S. Sasaki, S. Tarucha, S. M. Reimann, M. Koskinen, and M. Manninen, *Phys. Rev. B.*, 60:11514, 1999.

[3] T. Ezaki, N. Mori, and C. Hamaguchi, *Phys. Rev. B.*, 56:6428, 1997.

[4] M. Fujito, A. Natori, and H. Yasunaga, *Phys. Rev. B.*, 53:9952, 1996.

[5] A. Wojs and P. Hawrylak, *Phys. Rev. B.*, 53:10841, 1996.

[6] M. Koskinen, M. Manninen, and S. M. Reimann, *Phys. Rev. Lett.*, 79:1389, 1997.

[7] K. Hirose and N. S. Wingreen, *Phys. Rev. B., 59:4604, 1999.*

[8] In-Ho Lee, V. Rao, R. M. Martin, J.-P. Leburton, *Phys. Rev. B.*, 57(15):9035, 1998.

[9] V. Fock, *Z. Phys., 47:446, 1928.*

[10] C. G. Darwin, *Proc. Cambridge Philos. Soc.*, 27:86, 1930.

[11] B. Tanatar and D. M. Ceperley, *Phys. Rev. B.*, 39:5005, 1989.

[12] C. Attaccalite, S. Moroni, P. Gori-Giogi, and G. B. Bachelet, *Phys. Rev. Lett.*, 88:256601, 2002.

[13] E. Schrodinger, *Ann. der Phys.*, 79:361, 1926.

[14] V. Fock, *Z. Phys.*, 48:73, 1930.

[15] D. R. Hartree, *Proc. Cambrige Philos. Soc.*, 24:89, 1928.

[16] L. Cohen and C. Frishberg, *Phys. Rev. A.*, 13(3), 1976.

[17] L. H. Thomas, *Proc. Cambridge. Philos. Soc.*, 23:542, 1927.

[18] E. Fermi, *Z. Phys.*, 48:73, 1928.

[19] R. O. Jones and O. Gunnarsson, *Rev. Mod. Phys.*, 61(33):690, 1989.

[20] P. Hohenberg and W. Kohn, *Phys. Rev.*, 136:B864, 1964.

[21] W. Kohn, *Rev. Mod. Phys.*, 71(5): 1253, 1999.

[22] W. Kohn, In *the International School of Physics*, Course LXXXIX, page 4, 1985.

[23] R. M. Dreizler, E.K.U. Gross, *Density Functional Theory, An Approach to 0uantum Many-Body Problem*, Berlin Heidelberg: Springer-Verlag, 1990.

[24] M. Levy, *Proc. Natl. Acad. Sci. USA*, 76:6062, 1979.

[25] E. H. Lieb, ed. by A. Shimony and H. Feshbach, in *Physics as Natural Philosophy*, Cambridge: MIT Press, 1982.

[26] M. Levy, *Phys. Rev. A.*, 26:1200, 1982.

[27] W. Kohn and L. J. Sham, *Phys. Rev.*, 140:A1133, 1965.

[28] U. von Barth and L. Hedin, *J. Phys. C.*, 5:1629, 1972.

[29] M. M. Pant and A. K. Rajagopal, *Solid State Commun.*, 10:1157, 1972.

[30] A. K. Rajagopal and J. Callaway, *Phys. Rev. B.*, 7:1912, 1973.

[31] J. Singh, *Quantum Mechanics, Fundamentals and Applications to Technology*,

New York: John Wiley & Sons, Inc., 1997.

[32] J. Weis, R. J. Haug, K. V. Klitzing, and K. Ploog, *Phys. Rev. Lett.*, 71:4019, 1993.

[33] J. P. Perdew and Y. Wang, *Phys. Rev. B.*, 45:13244, 1992.

[34] S. Sahrakorpi, *Interface and Manual for Demonstrating the Schrodinger Wave Equation in Two Dimensions with Matlab*,Tampere University of Technology, Hp. Online, 1996. Available: http://alpha.cc.tut.fi/~sahrakor/research/teksti/teksti.html.

[35] S. O. Kasap, *Principles of Electrical Engineering Materials and Devices*, McGraw-Hill, 1997.

Appendices

Appendix A

The Effective-Mass Approximation

Recall that, in classical physics, we interpret mass as inertial resistance against acceleration per unit applied force (Newton's law of motion). When we treat the electron as a wave in Quantum mechanics we have to determine whether we can still, in some way, use the convenient classical relation $F = ma$ to describe the motion of an electron under an applied force such as eE, and if so what should be the apparent mass of the electron in crystal structures.

A theorem which enables us to apply classical law with quantum particle such as electrons is the **Ehrenfest theorem** named after P. Ehrenfest (1927). According to the theorem, the properties of a wavepacket representing a quantum particle can be determined from classical equations:

$$m\frac{d^2}{dt^2}\langle \mathbf{x} \rangle = -\left\langle \frac{\partial V}{\partial x} \right\rangle \tag{A.1}$$

The derivation of Eq. A.1 can be seen in quantum mechanic books. The Ehrenfest theorem is an extremely useful theorem in applied quantum mechanics because once the quantum problem is solved, the response of the particle to slowly varying external forces can be treated as if the particle is obeying classical equation.

We will now consider and evaluate the velocity and acceleration of the electron in conduction bands in response to an electric field, E_x, along $-x$ direction that imposes an external force $F_{ext} = eE_x$ in $+x$ direction, as shown in Figure A.1 [35].

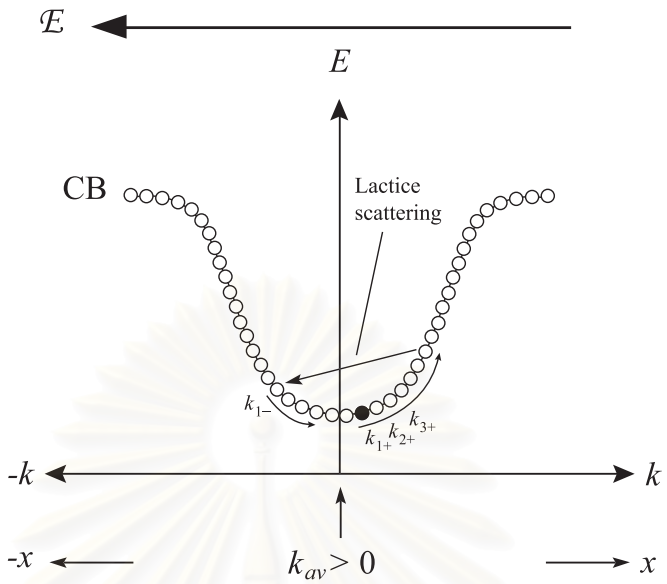

Figure A.1: In the presence of a field in the -x direction, the electron gains energy and increasing its k value along x until it is scattered to a random k value.

Our treatment will make use of the quantum mechanical E-k diagram of a crystal. Consider a wavepacket made up of wavefunctions near a particular k-value in a conduction band, the group velocity of this wavepacket representing an electron is defined as $\upsilon_g = d\omega/dk$ where ω is the frequency associated with the electron of energy E, i.e., $\omega = E/\hbar$, thus,

$$\upsilon_g = \frac{1}{\hbar}\frac{dE}{dk} \tag{A.2}$$

The group velocity is determined by the gradient of the E-k curve. In the presence of an electric field, the electron experiences a force $F_{ext} = eE_x$ from which it gains energy and moves up in the E-k diagram until it collides with a lattice vibration. During a small time interval, δt, between collisions, the electron moves a distance, $\upsilon_g t$, and hence gains energy, δE, which is

$$\delta E = F_{ext} \upsilon_g \delta t \tag{A.3}$$

We may also write, in general,

$$\begin{aligned} \delta E &= \frac{dE}{dk}\delta k \\ &= \hbar \upsilon_g \delta k \end{aligned} \tag{A.4}$$

Comparing the two equations for δE, we get

$$F_{ext}\delta t = \hbar \delta k \tag{A.5}$$

giving us the relation

$$F_{ext} = \hbar \frac{dk}{dt} \tag{A.6}$$

The term $\hbar k$ responds to the external forces as if it is the momentum of the electron, although, it is clear that $\hbar k$ contains the effects of the internal crystal potentials and is therefore not the true electron momentum [31].

The acceleration of the electron is defined as $d\upsilon_g/dt$ which is

$$\begin{aligned} a &= \frac{d}{dt}\left(\frac{1}{\hbar}\frac{dE}{dk}\right) \\ &= \frac{1}{\hbar}\frac{d^2E}{dk^2}\frac{dk}{dt} \\ &= \frac{F_{ext}}{\hbar^2}\frac{d^2E}{dk^2} \end{aligned} \tag{A.7}$$

We know that the response of a free electron to the external force is $F_{ext} = m_e a$, where m_e is the mass of electron in vacuum. Therefore, it is clear that from the last equality in Eq. A.7 that the effective mass of the electron in the crystal is

$$m_e^* = \hbar^2 \left[\frac{d^2E}{dk^2} \right]^{-1} \tag{A.8}$$

The electron responds to an external force and moves as if its mass were given by Eq. A.8. The effective mass obviously depends on the E-k relation which depends on the crystal structure. Its value is also different for electrons in the CB and for those in the VB, and moreover, it depends on the energy of the electron since it is related to the curvature of the E-k curve.

According to Eq. A.8 the effective mass of an electron can be both negative and positive quantities. When the electron is at the top of a band, i.e. the E-k curve is a downward concave, the effective mass of an electron at these energies in a band is then negative. That means the electron accelerate in the opposite direction to the applied external force, F_{ext}. On the other hand, the electron at the bottom of the CB has positive effective mass which is normally small compare to those at the middle of the band.

It should be stressed that Eq. A.8 defines the meaning of the effective mass in quantum mechanics. Its usefulness lies in the fact that we can measure it experimentally. This means we can simply replace m_e by m_e^* in equations that describe the effect of an external field on electron transport in crystal structures.

Appendix B

Rescaled Atomic Units and Conversion Factors

In this thesis, rescaled atomic units are used thoughout with lengths in units of effective Bohr radius,

$$a_0^* = \frac{4\pi\epsilon\hbar^2}{m^* e^2} \tag{B.1}$$

and energy in effective atomic units of energy called Hartree*,

$$E_a^* = \frac{e^2}{4\pi\epsilon a_0^*} \tag{B.2}$$

where m^* is the effective mass, ϵ is the dielectric constant. For a GaAs quantum dot $m^* = 0.065m_e$ and $\epsilon = 12.9\epsilon_0$.

B.1 Physical Constants

electron charge	e	$1.60217733 \times 10^{-19}C$
permittivity of vacuum	ϵ_o	$8.854187817 \times 10^{-12}$ $C^2N^{-1}m^{-2}$
electron mass	m_e	$9.1093897 \times 10^{-31}kg$
Planck s constant	h	$6.6260755 \times 10^{-34}Js$
Planck s constant	$\hbar$	$1.05457266 \times 10^{-34}Js$

B.2 Conversion factors

effective mass of electron	m^*	$5.9211033 \times 10^{-32}$ kg
effective Bohr radius	a_0^*	10.502133 nm
effective Hartree energy	E_a^*	$1.7029243 \times 10^{-21}$ J = 10.628812 meV

Bohr radius	a_0	$0.529177249 \times 10^{-10}m$
Hartree energy	$\frac{e^2}{4\pi\epsilon_0 a_0}$	$4.3597482 \times 10^{-18}J$

Appendix C

Matlab Code

```
function [EtotN,Error] = KohnSham(N,Nup,eigmax,eigmax2)
%
% "KohnSham.m" solves Kohn-Sham equations
%
% Usage: [EtotN,Error] = KohnSham(N,Nup,eigenmax,eigmax2)
%
% N:   The number of electrons
% Nup: The number of spin-up electrons
%
% eigmax:  the maximum eigenvalues to be counted in the first
calculation
% eigmax2: the maximum eigenvalues to be counted in the self-
% consistent LOOP
%
% Examples: Harmonic Confinement with k = 0.3
% If N<3, eigmax  = 1.3, eigmax2 = 1.8;
% If N<7, eigmax  = 1.3, eigmax2 = 3.0;
% If N<11, eigmax  = 1.5, eigmax2 = 4.0;
% If N<15, eigmax  = 1.7, eigmax2 = 5.0;
%
% the maximum of the eigenvalue is needed to be specified
% properly
% A larger eigmax or eigmax2 need more CPU-time to solve the self-
% consistent equations
%
% Confining potential can be changed in "potential.m"
% This M-files uses pde-toolbox
% Author: Khattiya Chalapat
% Year: 2003

Ndown = N-Nup;
time=cputime;           % this counts used CPU-time
stopplot = 9;

[gx0,gy0,gx1,gy1,gd,b]=data(N);
% define the coefficients of the Kohn-Sham equations
c = 0.5;
d = 1;

% geometry composition
dl      = decsg(gd);              % decompose geometry
[p,e,t] = initmesh(dl);           % initialize mesh
refine  = 2;
for i=1:refine
   [p,e,t]=refinemesh(dl,p,e,t);  % refine mesh
end

% Corner point indices
it1 = t(1,:);
it2 = t(2,:);
it3 = t(3,:);
```

```
% Find midpoints of triangles
x   = (p(1,it1)+p(1,it2)+p(1,it3))/3;
y   = (p(2,it1)+p(2,it2)+p(2,it3))/3;
% Initial Effective Potential
vp1 = potential(x,y);
% Vp2 can also be chosen to be different from vp1
vp2 = vp1;
[psiUp,EUp]=pdeeig1(b,p,e,t,c,vp1,d,[-Inf eigmax]);
[psiDown,EDown]=pdeeig1(b,p,e,t,c,vp2,d,[-Inf eigmax]);

% Find areas of triangles
[ar,a1,a2,a3] = pdetrg(p,t);

% Find normalization factor
if N>stopplot,
     Nnorm=N;
else
  Nnorm=stopplot;
end
normfac2Up   = NormFac(psiUp,Nnorm,ar,it1,it2,it3);
normfac2Down = NormFac(psiDown,Nnorm,ar,it1,it2,it3);

% Electron densities
nUp = nMidpoint(psiUp,normfac2Up,Nup,it1,it2,it3);
if Ndown ~= 0,
     nDown = nMidpoint(psiDown,normfac2Down,Ndown,it1,it2,it3);
else
     nDown = 0
end
n = nUp+nDown;

% classical electrostatic potential
ves = Ves(n,ar,x,y);

[vxUp,vxDown,Ex] = spinVx(nUp,nDown,n);
% correlation energy
[vcUp,Ec]   = spinVc(nUp,nDown,n,1);
[vcDown,Ec] = spinVc(nUp,nDown,n,-1);

%Confining potential
vp = potential(x,y);

%effective potential
veffUp   = vp+ves+vcUp+vxUp;
veffDown = vp+ves+vcDown+vxDown;

% iteration
iter  = 0;
EtotO = 0;
Err   = 1;
Error = [];
```

```
stopiter=0.0001;
checkdiv = 'converge';
while Err > stopiter
  clear psi;
  [psiUp,EnewUp]    =pdeeig1(b,p,e,t,c,veffUp,d,[-Inf eigmax2]);
  [psiDown,EnewDown]=pdeeig1(b,p,e,t,c,veffDown,d,[-Inf eigmax2]);

  EUp   = EnewUp;
  EDown = EnewDown;

  EesO  = sum(n(1,:).*ves(1,:).*ar(1,:));
  Vc    = sum(nUp(1,:).*vcUp(1,:).*ar(1,:))...
          +sum(nDown(1,:).*vcDown(1,:).*ar(1,:));
  Vx    = sum(nUp(1,:).*vxUp(1,:).*ar(1,:))...
          +sum(nDown(1,:).*vxDown(1,:).*ar(1,:));

  %Find normalization factor
  normfac2Up   = NormFac(psiUp,Nnorm,ar,it1,it2,it3);
  normfac2Down = NormFac(psiDown,Nnorm,ar,it1,it2,it3);

  % electron density
  nUp = nMidpoint(psiUp,normfac2Up,Nup,it1,it2,it3);

  if Ndown==0;,
    nDown=0;
  else
    nDown = nMidpoint(psiDown,normfac2Down,Ndown,it1,it2,it3);
  end

  n = nUp+nDown;

  vesO      = ves;
  vcUpO     = vcUp;
  vcDownO   = vcDown;
  vxUpO     = vxUp;
  vxDownO   = vxDown;
  % new correlation energy
    [vcUp,Ec]   = spinVc(nUp,nDown,n,1);
    [vcDown,Ec] = spinVc(nUp,nDown,n,-1);
    % new exchange energy
  [vxUp,vxDown,Ex] = spinVx(nUp,nDown,n);

  Eexc  = sum(n(1,:).*Ex(1,:).*ar(1,:));
  Ecor  = sum(n(1,:).*Ec(1,:).*ar(1,:));

  %electrostatic potential: direct integration
  ves  = Ves(n,ar,x,y);
  EesN = 0.5*sum(n(1,:).*ves(1,:).*ar(1,:));

  EtotN = sum(EUp(1:Nup))+sum(EDown(1:Ndown))-EesO-Vc+Vx+Ecor...
+Eexc+EesN
```

```
    Err   = abs(EtotN-EtotO);
    Error = [Error Err];
  EtotO = EtotN;
    iter  = iter +1;
    if iter>15,
    break;
    checkdiv = 'diverge';
  end

    % new effective potential
    ves    = 0.8*vesO+ 0.2*ves;
    vcUp   = 0.8*vcUpO+0.2*vcUp;
    vcDown = 0.8*vcDownO+0.2*vcDown;
  vxUp   = 0.8*vxUpO+0.2*vxUp;
  vxDown = 0.8*vxDownO+0.2*vxDown;

    veffUp   = vp+ves+vcUp+vxUp;
    veffDown = vp+ves+vcDown+vxDown;

end

% One-Particle Eigen Functions and Energies Plot
EigenPlot(psiUp,EUp,normfac2Up,p,e,t,gx0,gx1,gy0,gy1,stopplot,time)
EigenPlot(psiDown,EDown,normfac2Down,p,e,t,gx0,gx1,gy0,gy1,stopplot,time)
myplot1(p,e,t,n,EtotN,N,Nup,checkdiv);

figure;
subplot(2,1,1)
pdeplot(p,e,t,'zdata',nUp,'xydata',nUp,'mesh','on','colorbar','off','colormap',[1 1 1]);
title(sprintf('nUp, Nup= %3.0f, Etot= %f',Nup,EtotN));
subplot(2,1,2)

if N~=Nup,
  pdeplot(p,e,t,'zdata',nDown,'xydata',nDown,'mesh','on','colorbar',
'off','colormap',[1 1 1]);
    title(sprintf('nDown, Ndown= %3.0f, Etot= %f',N-Nup,EtotN));
end

% Save the values of each quantities in a text file
Data = fopen('C:\MATLABR11\work\...\data1.txt','w');  % Set Path
fprintf(Data,'\nN=%3.0f,  Nup=%3.0f, Etot=%f, Ees=%f, Ex=%f, ...
Ecor =%f, Vx=%f, Vc=%f',N,Nup,EtotN,EesN,Eexc,Ecor,Vx,Vc);
fclose(Data);

return
```

```
function [gx0,gy0,gx1,gy1,gd,b]=data(N)

% define rectangular GEOMETRY
gx0=-15;                    % left lower corner
gy0=-15;
gx1=15;                     % right upper corner
gy1=15;

% geometry description matrix; counterclockwise ( see descg )
gd=[1 0 0 15]';      % circle xcenter ycenter radius

% BOUNDARY conditions ( see assemb )
b=[1 1 1 1 1 1 '0' '0' '1' '0']';     % q g h r
b=[b b b b];

return
```

```
function f = potential(x,y)
%
% potential.m determines the values of confining potential on 2D meshes
% V = 0.5*k^2*(delta*x^2+(1/delta)*y^2)
% k^2 -> k2  adjusting this parameter will change widths and depths of the confining potential
% Harmonic Potential: delta = 1
% Parabolic Potential: delta > 1
%
% f can be any analytic functions
%
% After changing the parameter values in this file,
% the parameters in "data.m" may also needed to be changed.
%
% Author: K. chalapat
% Year: 2003

delta = 1;
k2    = 0.09;
f     = 0.5*k2*(delta*x.^2+(1/delta)*y.^2);

return
```

```
function [v,l]=pdeeig1(b,p,e,t,c,a,d,r)
%
% "pdeeig1.m" is the same as "pdeeig.m" in pdetool
% the difference is the function assema1 in line 32:
% [K,M,unused3] = assema1(p,t,c,a,zeros(N,1));
%
% by K. Chalapat
% 2003
%
%PDEEIG Solve eigenvalue PDE problem.
%
% [V,L]=PDEEIG(B,P,E,T,C,A,D,R) produces the solution to the
% FEM formulation of the PDE eigenvalue problem
% -div(c grad(u))+a u=l d u, on a geometry described by
% P, E, and T, and with boundary conditions given by B.
%
% R is a two element vector, indicating an interval on the
% real axis. (The left-hand side may be -Inf.)
% The algorithm returns all eigvalues in this interval in L.
%
% V is a matrix of eigenvectors. For the scalar case each
% column in V is an eigenvector of solution values at the
% corresponding node points from  P. For a system of dimension % N
with NP node points, the first NP rows of V describe the
% first component of v, the following NP rows of V describe
% the second component of v, and so on. Thus, the components
% of v are placed in blocks V as N blocks of node point rows.
%

if nargin==8,
      np = size(p,2);
      % Boundary contributions
      [Q,unused1,H,unused2] = assemb(b,p,e);
   % Number of variables
   N = size(Q,2)/np;
   [K,M,unused3] = assema1(p,t,c,a,zeros(N,1));
      [K,unused1,B,unused2] = assempde(K,M,unused3,Q,unused1,H,unused2);
      [unused,M]    = assema(p,t,0,d,zeros(N,1));
elseif nargin==4,
      K = b;
      B = p;
      M = e;
      r = t;
else
   error('number of input argument must be 4 or 7');
end

M=B'*M*B;

if r(1)~=-Inf
      spd       = 1; % We assume ...
else
```

```
    spd = 0;
end

[v,l,ires] = sptarn(K,M,r(1),r(2),spd);

if ires<0,
    disp('Warning: there may be more eigenvalues in the interval');
end

if ~isempty(v)
    v = B*v;
end
```

```
function normfac2 = NormFac(psi,Nnorm,ar,it1,it2,it3)
%
% "NormFac.m" calculate normalization factor for the
%  eigenvectors: "psiUp" and "psiDown"
%
% (Normalization Factor)^2 = normfac2
%
% by K. Chalapat
% 2003
%
for i = 1:Nnorm
     temp(:,i)  = psi(:,i).^2;
end
temp2 = temp';
for i = 1:Nnorm
   % values at midpoints of triangles
   midpoint_psi2(i,:) = (temp2(i,it1)+temp2(i,it2)...
                                          +temp2(i,it3))/3;
   normfac2(i) = sum(ar.*midpoint_psi2(i,:));
   % normalized wavefunction = psi/sqrt(normfac2)
end
clear temp temp2 midpoint_psi2;

return
```

```
function n2 = nMidpoint(psi,normfac2,N,it1,it2,it3)
%
% "nMidpoint.m" calculates the electron density at
% the midpoints of triangles
%
% by K. Chalapat
% 2003
%
n = 0;
for i = 1:N
   n = n + (psi(:,i).^2)/normfac2(i);
end
n = n';
% electron density at midpoints of triangles
n2 = (n(1,it1)+n(1,it2)+n(1,it3))/3;

return
```

```
function ves = Ves(n,ar,x,y)
%
% "Ves.m" calculates the Hartree (Classical Electrostatic)
% potential
% by using direct integration
%
% by K. Chalapat
% 2003
%
Npoint = size(x,2);
ves(1,1) = n(1,1)*3.53.*sqrt(ar(1,1))+sum((n(1,2:Npoint).*
ar(1,2:Npoint))./sqrt( (x(1,2:Npoint)-x(1,1)).^2+(y(1,2:Npoint)-
y(1,1)).^2 ));
for j=2:Npoint-1
   ves(1,j) = n(1,j)*3.53.*sqrt(ar(1,j))+sum((n(1,1:j-1).*
ar(1,1:j-1))./sqrt( (x(1,1:j-1)-x(1,j)).^2
+(y(1,1:j-1)-y(1,j)).^2 ));
   ves(1,j) = ves(1,j)+sum((n(1,j+1:Npoint).*ar(1,j+1:Npoint))./
sqrt((x(1,j+1:Npoint)-x(1,j)).^2+(y(1,j+1:Npoint)-y(1,j)).^2 ));
end
ves(1,Npoint) = n(1,Npoint)*3.53.*sqrt(ar(1,Npoint))+
sum((n(1,1:Npoint-1).*ar(1,1:Npoint-1))./sqrt( (x(1,1:Npoint-1)-
x(1,Npoint)).^2+(y(1,1:Npoint-1)-y(1,Npoint)).^2 ));

return
```

```
function [VxUp,VxDown,Ex] = spinVx(nUp,nDown,n)
%
% "spinVx.m" defines the Exchange Energy on mesh points
%
% by K. Chalapat
% 2003

r = 1./sqrt(pi*n);     % density parameter
Pz = (nUp-nDown)./n;
A      = 2*sqrt(2)/(3*pi);
Ex     = -A*( (1+Pz).^(3/2)+(1-Pz).^(3/2) )./r;
dExdrs = A*( (1+Pz).^(3/2)+(1-Pz).^(3/2) )./r.^2;
dExdPz = -sqrt(2)*(sqrt(1+Pz)-sqrt(1-Pz))./(pi*r);
VxUp   = Ex-0.5*r.*dExdrs-(Pz-1).*dExdPz;
VxDown = Ex-0.5*r.*dExdrs-(Pz+1).*dExdPz;

return
```

```
function [Vc,Ec] = spinVc(nUp,nDown,n,sgn)
%
% "spinVc.m" defines Correlation Potential
% of Attaccalite et al (2002) on mesh points
%
% by K. Chalapat
% 2003
%

rs = 1./sqrt(pi*n);         %density parameter
Pz = (nUp-nDown)./n;  %Polarization

A0 = -0.1925;
B0 = 0.0863136;
C0 = 0.057234;
E0 = 1.0022;
F0 =-0.02069;
G0 = 0.340;
H0 = 1.747e-2;
D0 = -A0*H0;

A1 = 0.117331;
B1 = -3.394e-2;
C1 = -7.66765e-3;
E1 = 0.4133;
G1 = 6.68467e-2;
H1 = 7.799e-4;
D1 = -A1*H1;

A2 = 0.0234188;
B2 = -0.037093;
C2 = 0.0163618;
E2 = 1.424301;
H2 = 1.163099;
D2 = -A2*H2;

Beta = 1.3386;
a    = 2*sqrt(2)/(3*pi);

Fn0    = E0*rs+F0*rs.^(1.5)+G0*rs.^2+H0*rs.^3;
alpha0 = A0+(B0*rs+C0*rs.^2+D0*rs.^3).*log(1+1./Fn0);
Fn1    = E1*rs+G1*rs.^2+H1*rs.^3;
alpha1 = A1+(B1*rs+C1*rs.^2+D1*rs.^3).*log(1+1./Fn1);
Fn2    = E2*rs+H2*rs.^3;
alpha2 = A2+(B2*rs+C2*rs.^2+D2*rs.^3).*log(1+1./Fn2);

%Correlation energy / Particle
Fn     = (1+Pz).^(1.5)+(1-Pz).^(1.5)-2-0.75*Pz.^2-(3/64)*Pz.^4;
Ec     = a*(1-exp(-Beta*rs)).*Fn./rs +alpha0+alpha1.*Pz.^2+alpha2.*Pz.^4;
```

```
dFn0    = E0+1.5*F0*sqrt(rs)+2*G0*rs+3*H0*rs.^2;
dalpha0 = (B0+2*C0*rs+3*D0*rs.^2).*log(1+1./Fn0)-
(B0*rs+C0*rs.^2+D0*rs.^3).*dFn0./(Fn0.*(Fn0+1));
dFn1    = E1+2*G1*rs+3*H1*rs.^2;
dalpha1 = (B1+2*C1*rs+3*D1*rs.^2).*log(1+1./Fn1)-
(B1*rs+C1*rs.^2+D1*rs.^3).*dFn1./(Fn1.*(Fn1+1));
dFn2    = E2+3*H2*rs.^2;
dalpha2 = (B2+2*C2*rs+3*D2*rs.^2).*log(1+1./Fn2)-
(B2*rs+C2*rs.^2+D2*rs.^3).*dFn2./(Fn2.*(Fn2+1));
dEcdrs  = (a./(rs.^2)).*Fn.*(exp(-Beta*rs).*(1+Beta*rs)-
1)+dalpha0+dalpha1.*Pz.^2+dalpha2.*Pz.^4;

dFn     = 1.5*(sqrt(1+Pz)-sqrt(1-Pz))-(1.5)*Pz-3*(Pz.^3)/16;
dEcdPz  = (a./rs).*dFn.*(1-exp(-Beta*rs))+2*alpha1.*Pz+4*alpha2.*Pz.^3;

%Correlation Potential / Particle
Vc      = Ec-0.5*rs.*dEcdrs-(Pz-sgn).*dEcdPz;

return
```

```
function f = potential(x,y)
%
% potential.m determines the values of confining potential on 2D meshes
% V = 0.5*k^2*(delta*x^2+(1/delta)*y^2)
% k^2 -> k2  adjusting this parameter will change widths and depths of the confining potential
% Harmonic Potential: delta = 1
% Parabolic Potential: delta > 1
%
% f can be any analytic functions
%
% After changing the parameter values in this file,
% the parameters in "data.m" may also needed to be changed.
%
% Author: K. chalapat
% Year: 2003

delta = 1;
k2    = 0.09;
f     = 0.5*k2*(delta*x.^2+(1/delta)*y.^2);

return
```

```
function EigenPlot(psi,E,normfac2,p,e,t,gx0,gx1,gy0,gy1,...
                                    stopplot,time)
%
% "EigenPlot.m" plots eigenstates and eigenvectors of
% the Kohn-Sham equations
%
elapsed=cputime-time;
fig1 = figure;
set(fig1,'papertype','a4letter','paperorientation','landscape')
if size(psi,2)>=9
  stop=stopplot;
else
    stop=size(psi,2);
end
step=1;
loop=1;
for i=1:step:stop
  subplot(3,3,loop)
    pdeplot(p,e,t,'xydata',(psi(:,round(i)).^2)/normfac2(i),'mesh',
'off','colormap','gray','colorbar','off');
    axis([gx0 gx1 gy0 gy1])
  %axis('square')
  grid on
    if i==1
        title(sprintf('CPU-time %7.3f s, E = %6.5f', elapsed,
E(round(i))))
  else
        title(sprintf('E = # %3.0f = %6.5f',round(i),E(round(i))))
    end
  loop=loop+1;
end

return
```

```
function myplot1(p,e,t,n,Etot,N,Nup,checkdiv);
%
% "myplot1.m" plots Electron Density in 3D and 2D space
%
% by K. Chalapat
% 2003
%
figure;
pdeplot(p,e,t,'zdata',n,'xydata',n,'mesh','on','colorbar','off',
'colormap',[1 1 1]);
title(sprintf('Electron Density, N = %3.0f, Nup = %3.0f, Etot = %f, "%s"',N,Nup,Etot,checkdiv));
figure;
pdeplot(p,e,t,'xydata',n,'mesh','off');
title(sprintf('Electron Density, N = %3.0f, Nup = %3.0f',N,Nup));

return
```

```
function [ks,km,fm]=assema1(p,t,c,a,f,u,time,sdl)
%
% the difference between "assema1.m" and "assema.m" in pdetool
% is the function: pdeasma1 in line 158
%
% by K. Chalapat
% 2003
%
%ASSEMA Assembles area integral contributions in a PDE problem.
%
% [K,M,F1]=ASSEMA(P,T,C,A,F) assembles the stiffness matrix K,
% the mass matrix M, and the right-hand side vector F1.
%
gotu    = 0;
gottime = 0;
gotsdl  = 0;

if nargin==5
   % No action
elseif nargin==6
     if size(u,1)>1
     gotu = 1;
     else
     time    = u;
     gottime = 1;
     end
elseif nargin==7
     if size(u,1)>1
     gotu    = 1;
     gottime = 1;
     else
     sdl     = time;
     time    = u;
     gottime = 1;
     gotsdl  = 1;
     end
elseif nargin==8,
     gotu    = 1;
     gottime = 1;
     gotsdl  = 1;
else
     error('Wrong number of input arguments');
end

% Choose triangles to assemble
if gotsdl
     it = pdesdt(t,sdl);
     t  = t(:,it);
end

if ~gottime
```

```
    time = [];
end

nt = size(t,2); % Number of triangles
np = size(p,2); % Number of points

% Corner point indices
it1 = t(1,:);
it2 = t(2,:);
it3 = t(3,:);

% Triangle geometries:
[ar,g1x,g1y,g2x,g2y,g3x,g3y] = pdetrg(p,t);

% Find midpoints of triangles
x  = (p(1,it1)+p(1,it2)+p(1,it3))/3;
y  = (p(2,it1)+p(2,it2)+p(2,it3))/3;

sd = t(4,:);

if ~gotu,
    uu=[];
    u=[];
    ux=[];
    uy=[];
else
    uu = u;
    N  = length(uu)/np;
    uu = reshape(uu,np,N);
    u  = (uu(it1,:).'+uu(it2,:).'+uu(it3,:).')/3;
    ux = uu(it1,:).'.*(ones(N,1)*g1x)+uu(it2,:).'.*(ones(N,1)*g2x)+uu
(it3,:).'.*(ones(N,1)*g3x);
    uy = uu(it1,:).'.*(ones(N,1)*g1y)+uu(it2,:).'.*(ones(N,1)*g2y)+uu
(it3,:).'.*(ones(N,1)*g3y);
    uu = reshape(uu,np*N,1);
end

if ~gotu,
    % The number of variables IS the number of rows in F
  N = size(f,1);
end

% Stiffness matrix
c = pdetfxpd(p,t,uu,time,c);

if any(c(:)),
    ks  = sparse(N*np,N*np);
    nrc = size(c,1);
    if nrc>=1 & nrc<=4, % Block scalar c
    ks1 = pdeasmc(it1,it2,it3,np,ar,x,y,sd,u,ux,uy,time,g1x,g1y,g2x,g2y,g3x,g3y
,c);
```

```
    [ii,jj,kss] = find(ks1);
    for k=1:N,
        ks = ks+sparse(ii+(k-1)*np,jj+(k-1)*np,kss,N*np,N*np);
    end
    elseif nrc==N | nrc==2*N | nrc==3*N | nrc==4*N, % Block diagonal c
    nb = nrc/N;
    m1 = 1;
    m2 = nb;
    for k=1:N,
        ks1 =
pdeasmc(it1,it2,it3,np,ar,x,y,sd,u,ux,uy,time,g1x,g1y,g2x,g2y,g3x,g3y
,c(m1:m2,:));
        [ii,jj,kss] = find(ks1);
        ks = ks+sparse(ii+(k-1)*np,jj+(k-1)*np,kss,N*np,N*np);
        m1 = m1+nb;
        m2 = m2+nb;
    end
    elseif nrc==2*N*(2*N+1)/2, % Symmetric c
    m1 = 1;
    m2 = 4;
    for l=1:N,
        for k=1:l-1,
            ks1 =
pdeasmc(it1,it2,it3,np,ar,x,y,sd,u,ux,uy,time,g1x,g1y,g2x,g2y,g3x,g3y
,c(m1:m2,:));
            [ii,jj,kss] = find(ks1);
            ks = ks+sparse(ii+(k-1)*np,jj+(l-1)*np,kss,N*np,N*np);
            m1 = m1+4;
            m2 = m2+4;
        end
        m1 = m1+3;
        m2 = m2+3;
    end
    ks = ks+ks.';
    m1 = 1;
    m2 = 3;
    for k=1:N,
        ks1 =
pdeasmc(it1,it2,it3,np,ar,x,y,sd,u,ux,uy,time,g1x,g1y,g2x,g2y,g3x,g3y
,c(m1:m2,:));
        [ii,jj,kss] = find(ks1);
        ks = ks+sparse(ii+(k-1)*np,jj+(k-1)*np,kss,N*np,N*np);
        m1 = m1+3+4*k;
        m2 = m2+3+4*k;
    end
    elseif nrc==4*N*N, % General (unsymmetric) c
    m1=1;
    m2=4;
    for l=1:N,
        for k=1:N,
```

```
            ks1 =
pdeasmc(it1,it2,it3,np,ar,x,y,sd,u,ux,uy,time,g1x,g1y,g2x,g2y,g3x,g3y
,c(m1:m2,:));
            [ii,jj,kss]=find(ks1);
            ks = ks+sparse(ii+(k-1)*np,jj+(l-1)*np,kss,N*np,N*np);
            m1 = m1+4;
            m2 = m2+4;
        end
    end
    else
    error('Wrong number of rows of c');
    end % nrc
    clear c ks1;
else
    clear c;
    ks = sparse(N*np,N*np);
end

% Mass matrix
% a
km  = sparse(N*np,N*np);
km1 = pdeasma1(it1,it2,it3,np,ar,sd,u,ux,uy,time,a);
[ii,jj,kmm] = find(km1);
for k=1:N,
  km = km+sparse(ii+(k-1)*np,jj+(k-1)*np,kmm,N*np,N*np);
end
clear a km1;

% RHS
f = pdetfxpd(p,t,uu,time,f);

if any(f(:)),
    fm  = zeros(N*np,1);
    nrf = size(f,1);
    if nrf==1, % Scalar f
    fm1 = pdeasmf(it1,it2,it3,np,ar,x,y,sd,u,ux,uy,time,f);
    for k=1:N,
        fm((k-1)*np+1:k*np,:) = fm1;
    end
    elseif nrf==N, % Vector f
    for k=1:N,
    fm1 = pdeasmf(it1,it2,it3,np,ar,x,y,sd,u,ux,uy,time,f(k,:));
    fm((k-1)*np+1:k*np,:) = fm1;
    end
    else
    error('Wrong number of rows of f');
    end % size(f,1)
    clear f fm1;
else
    clear f;
    fm = zeros(N*np,1);
end
```

```
function M = pdeasma1(it1,it2,it3,np,ar,sd,u,ux,uy,time,a)
%
% The difference between "pdeasma1.m" and "pdeasma.m" in
% pdetool is that there is no use of the function "pdetexpd"
% in "pdeasma1.m"
%
% PDEASMA Assemble the A coefficient.
%
% by K. Chalapat
% 2003
%
avoid_arithmetics_on_NaNs = 0;
if ~isieee & any(isnan(time))
    % PARABOLIC and HYPERBOLIC probes with time=NaN for
    % explicit time dependence. We must not cause any floating point
    % exceptions in this case.
    avoid_arithmetics_on_NaNs = 1;
end

if avoid_arithmetics_on_NaNs & any(isnan(a))
    M = sparse(1,1,NaN,np,np);
    return
end
aod = a.*ar/12; % Off diagonal element
ad  = 2*aod; % Diagonal element
M   = sparse(it1,it2,aod,np,np);
M   = M+sparse(it2,it3,aod,np,np);
M   = M+sparse(it3,it1,aod,np,np);
M   = M+M.';
M   = M+sparse(it1,it1,ad,np,np);
M   = M+sparse(it2,it2,ad,np,np);
M   = M+sparse(it3,it3,ad,np,np);
```

Vitae

Khattiya Chalapat was born on August 13, 1978 in Bangkok. She received the Bachelor degree of Science in Physics from Chulalongkorn University in 1999. During her studying for the M.Sc. degree, she had a practical experience at Laser- und Medizin Technologie GmbH, Berlin, Germany, and participated in the Workshop on Correlation Effects in Electronic Structure Calculations at the Abdus Salam International Centre for Theoretical Physics, Trieste, Italy.